

Non-factorisable corrections to t -channel single-top production at the LHC

Chiara Signorile-Signorile

LFC22

Trento, 31/08/2022

In collaboration with: Christian Brønnum-Hansen, Kirill Melnikov, Jérémie Quarroz and Chen-Yu Wang
Based on: arXiv 2204.05770

Motivation: why top quark?

- Heaviest observed particle

$$- m_t = (173.34 \pm 0.76) \text{ GeV}$$

[World Combination 14, ATLAS, CDF, CMS, D0]

- Substantial Yukawa coupling

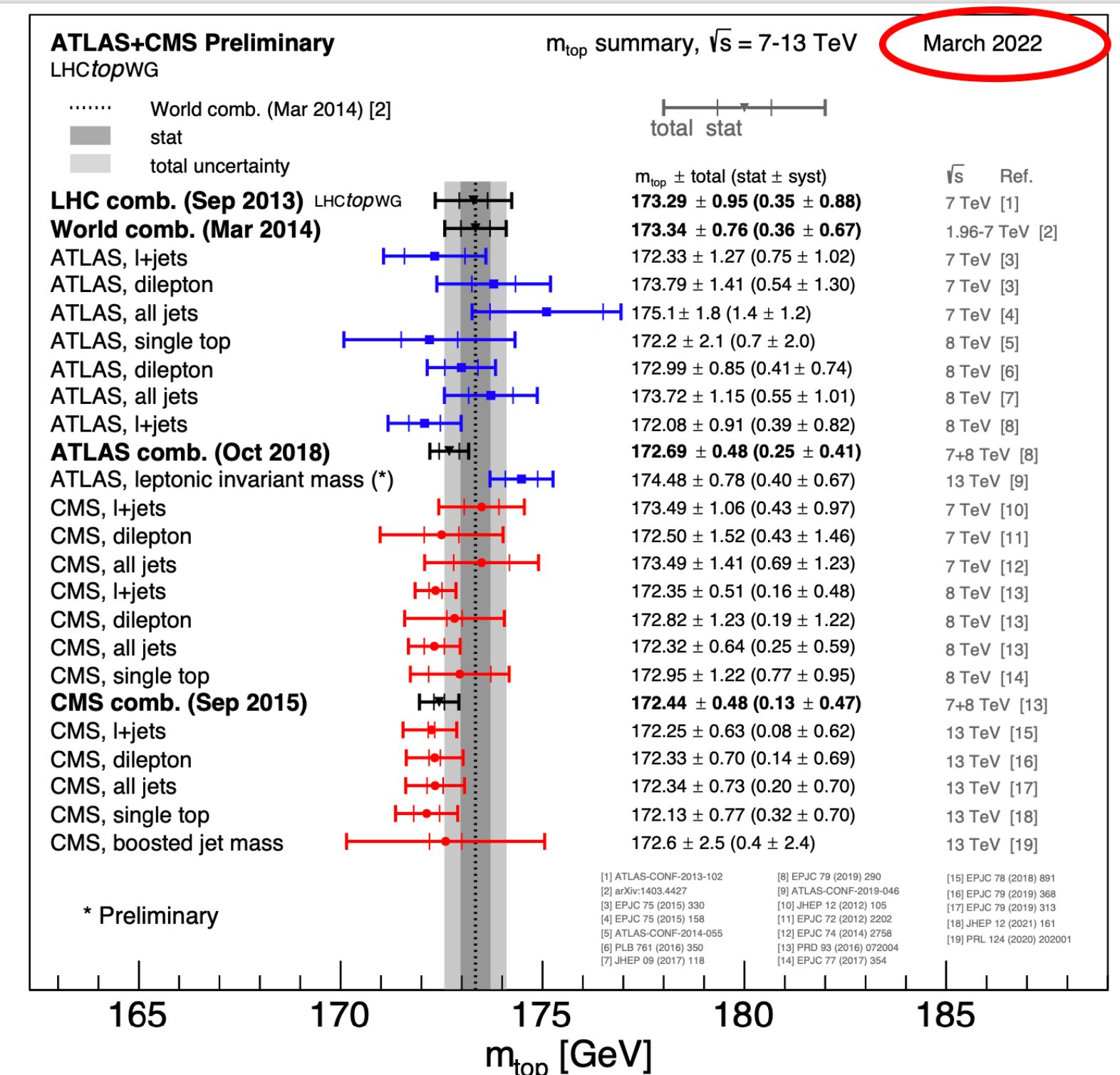
$$- Y_t = \sqrt{2} \frac{m_t}{v} \sim 1$$

- Special relation with SM Higgs Boson

- Short lifetime → decay before bound states can be formed

Precision top-quark Physics

- Extracting SM parameters
- Constraining PDFs
- Examining (anomalous) couplings
- Better understanding of EW symmetry breaking
- Hints for heavy New Physics



See Victor Miralles's talk!

Motivation: single-top production

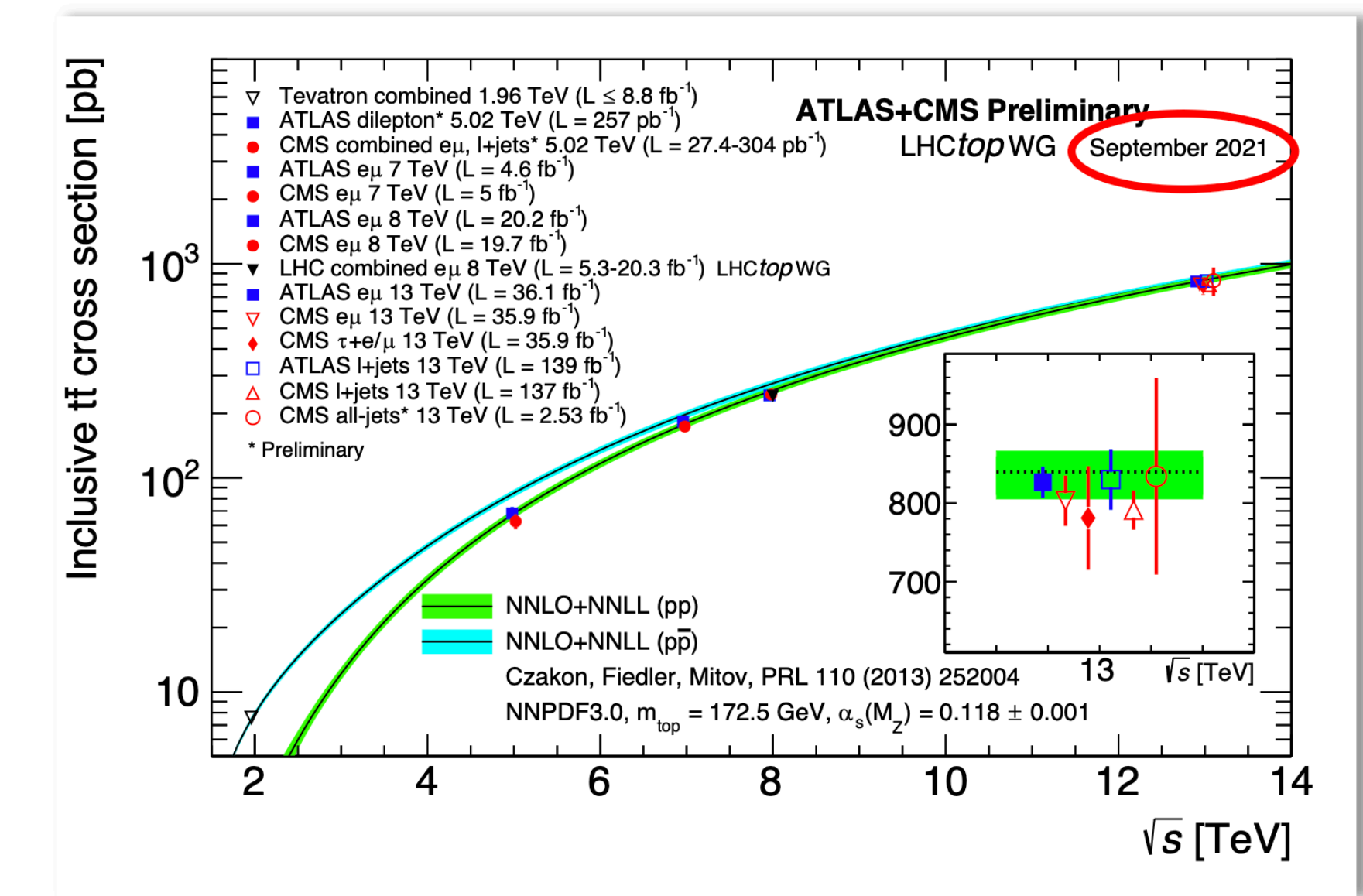
- At LHC top quarks are mainly produced in pairs via strong interactions

- Large production rate

- Advanced theoretical predictions:

NLO QCD [Nason, Dawson, Ellis '88] and NLO EW corrections [Kuhn, Scharf, Uwer '06]

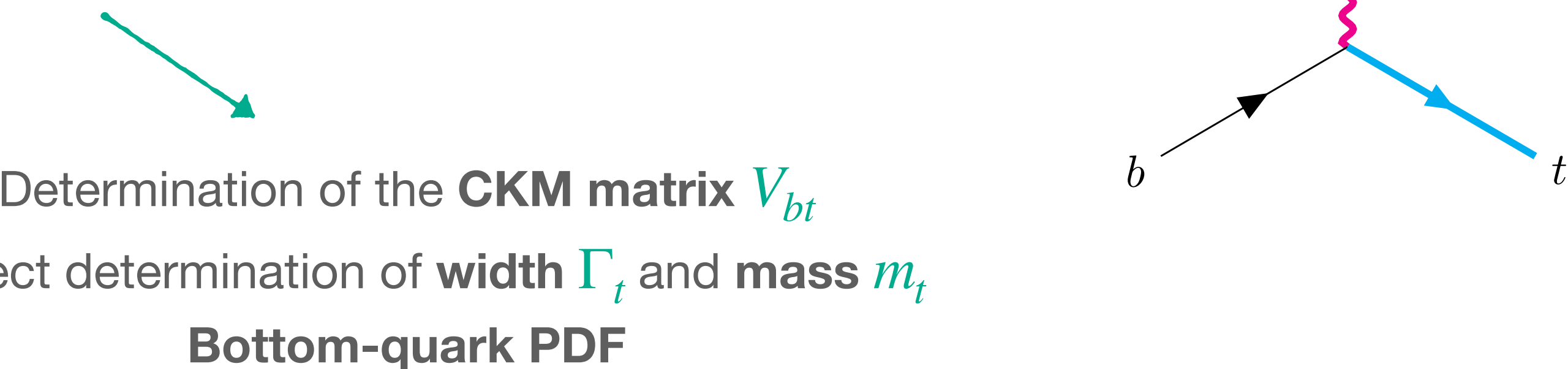
total and fully differential NNLO QCD corrections in the NW approximation
[Czakon, Fiedler, Mitov '13, Behring, Czakon, Mitov et al. '19, Czakon, Mitov, Poncelet '21]



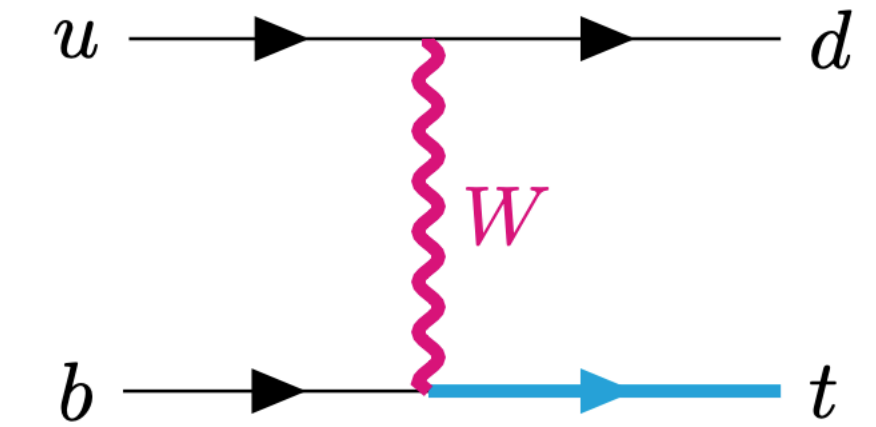
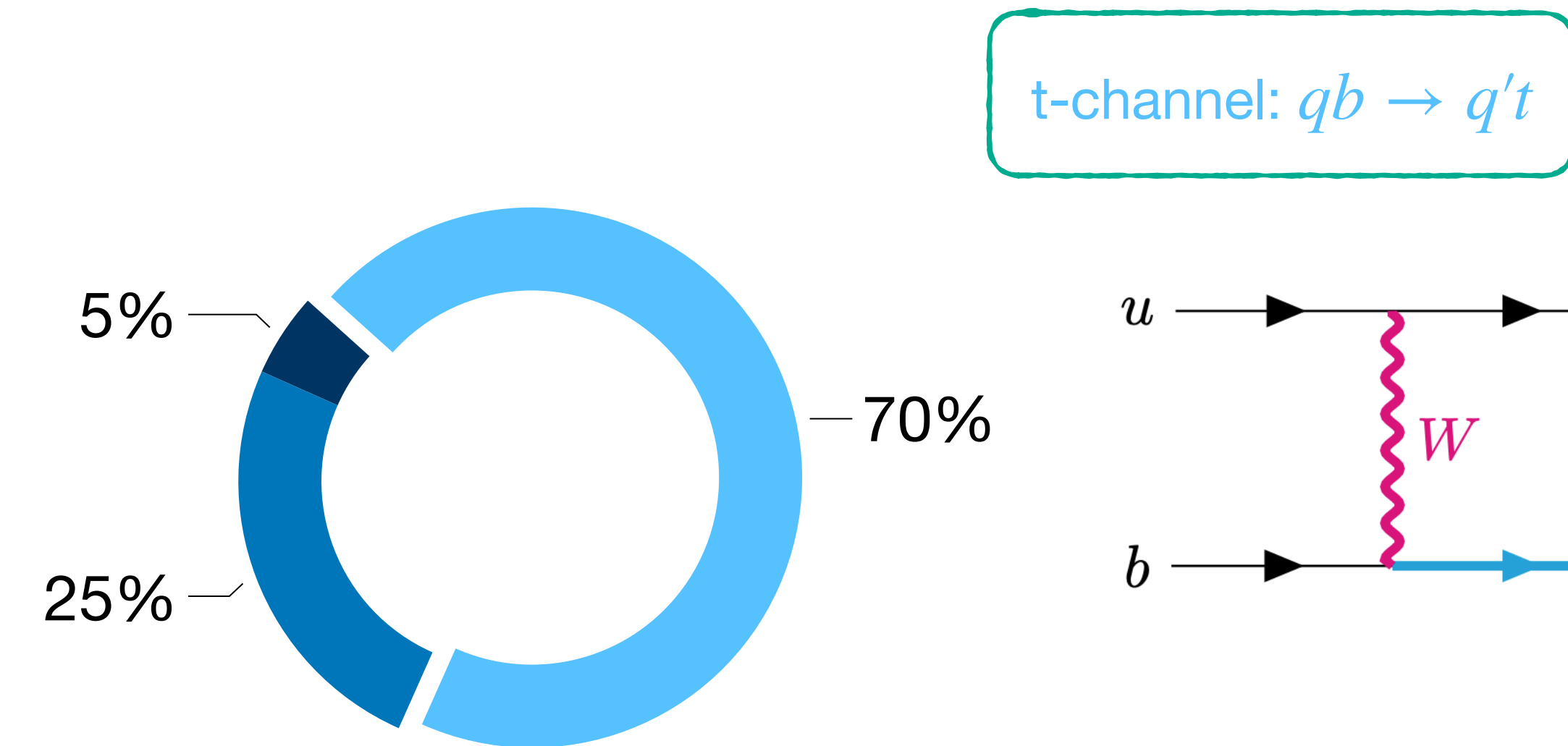
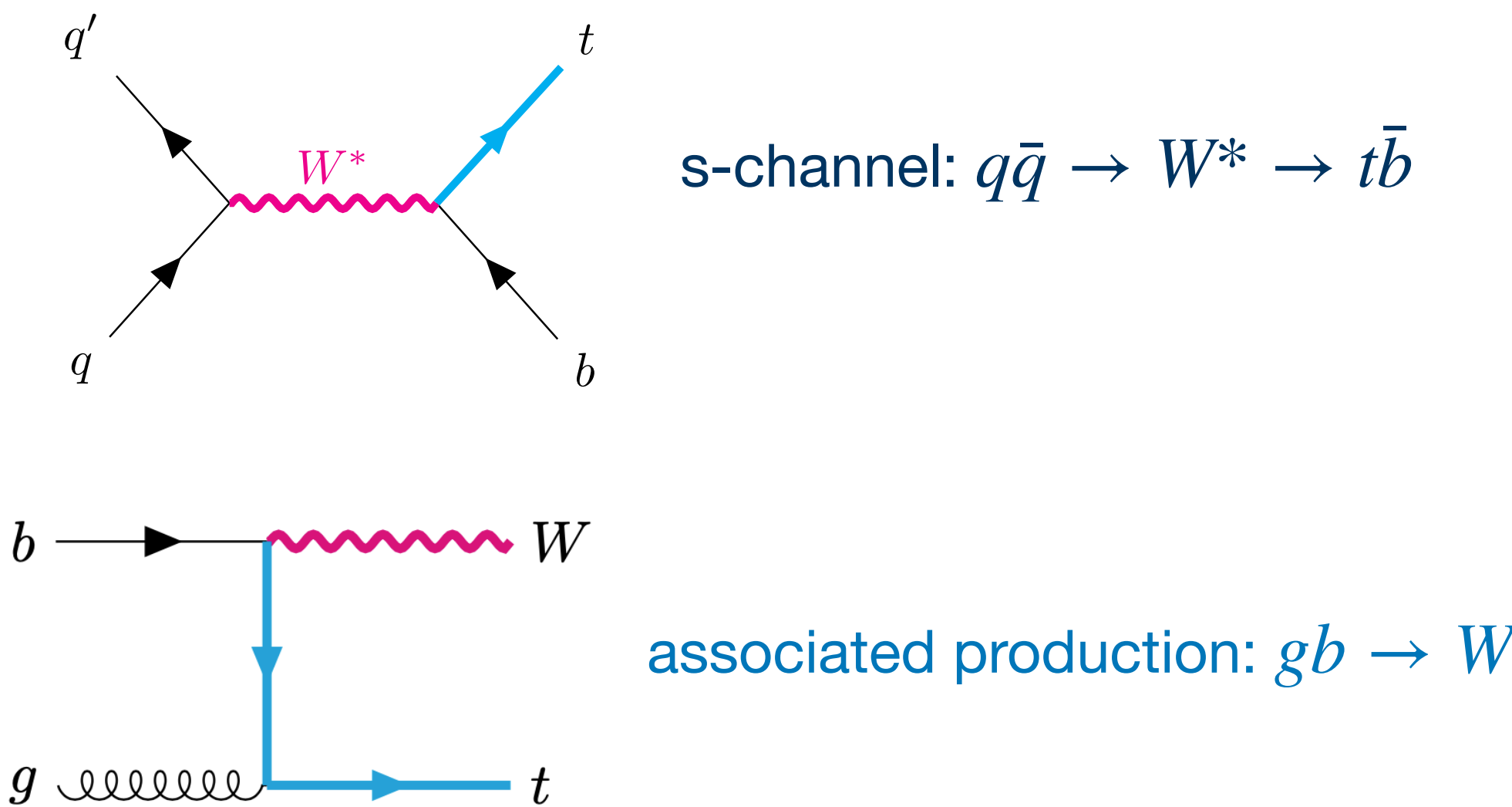
- Single-top production also relevant

- Production rate of the same order of magnitude as $t\bar{t}$: $\sigma_t \sim 1/4 \sigma_{t\bar{t}}$

- Electroweak mediated



Single-top production: different modes



- Two main topologies contribute to the t -channel, single-top production:

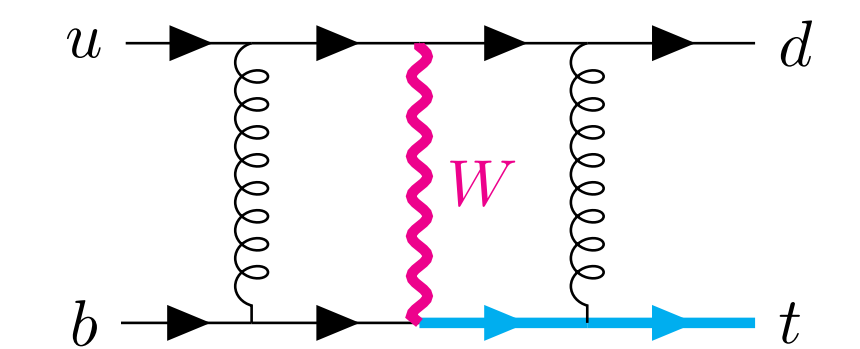
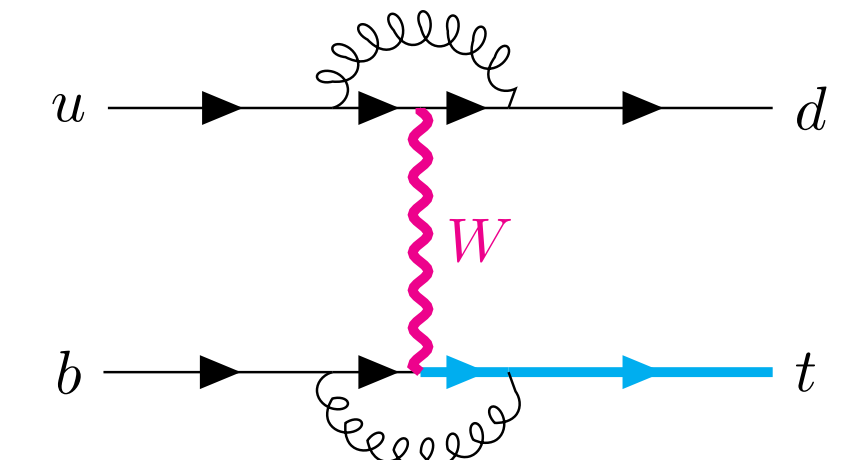
- **Factorisable contributions**

Extensively investigated:

NLO QCD [Bordes, van Eijk '95][Campbell, Ellis, Tramontano '04][Cao, Yuan '05][Cao, Schwienhorst, Benitez, Brock, Yuan '05][Harris, Laenen, Phaf, Sullivan, Weinzierl '02] [Schwienhorst, Yuan, Mueller, Cao '11]

NNLO QCD [Brucherseifer, Caola, Melnikov '14] [Berger, Gao, Yuan, Zhu '16] [Campbell, Neumann, Sullivan '21]

- **Non-factorisable contributions** → cross talk between different quark lines

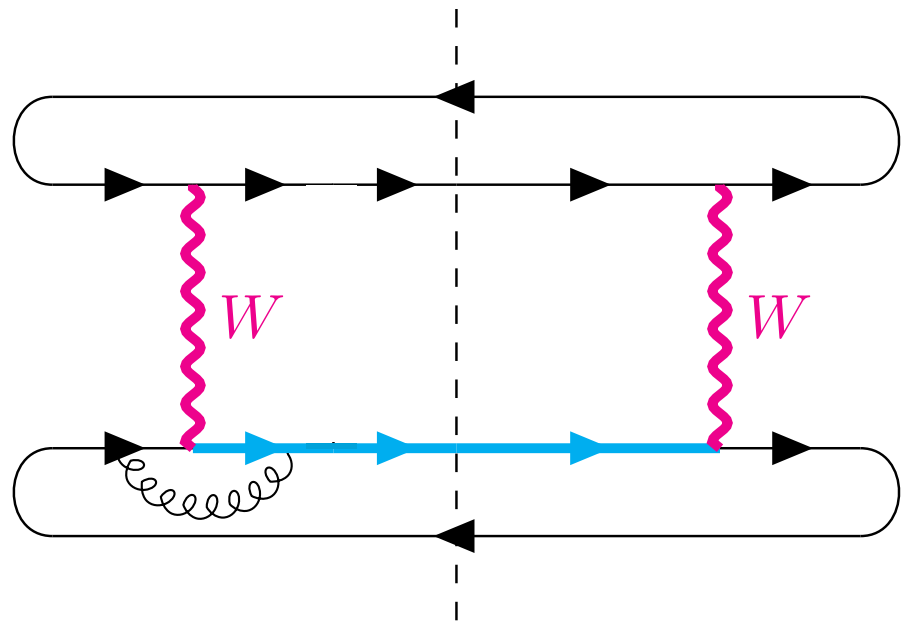


Factorisable vs non-factorisable corrections

[thanks to Jérémie and Christian
for the nice picture in the slides]

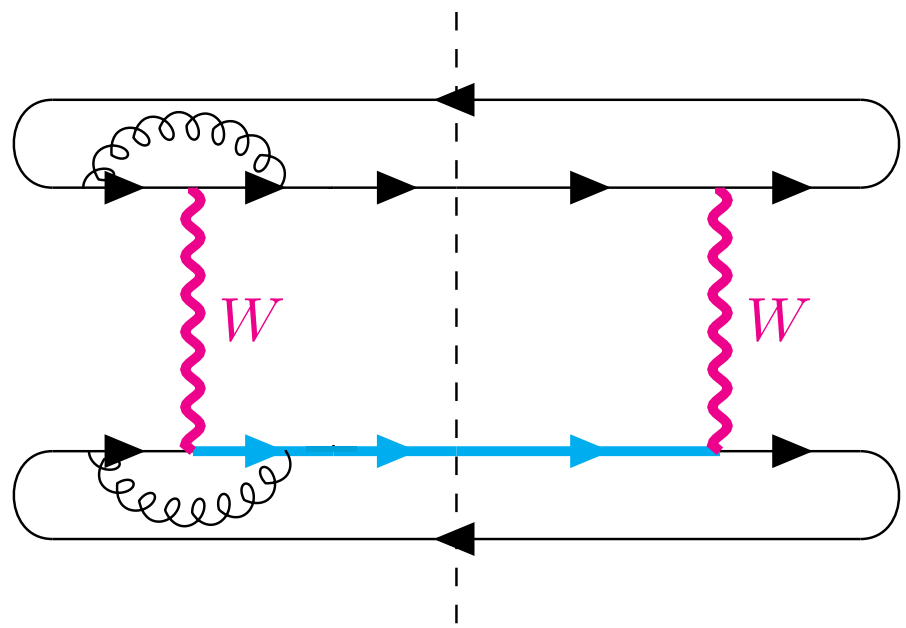
Factorisable contributions

NLO



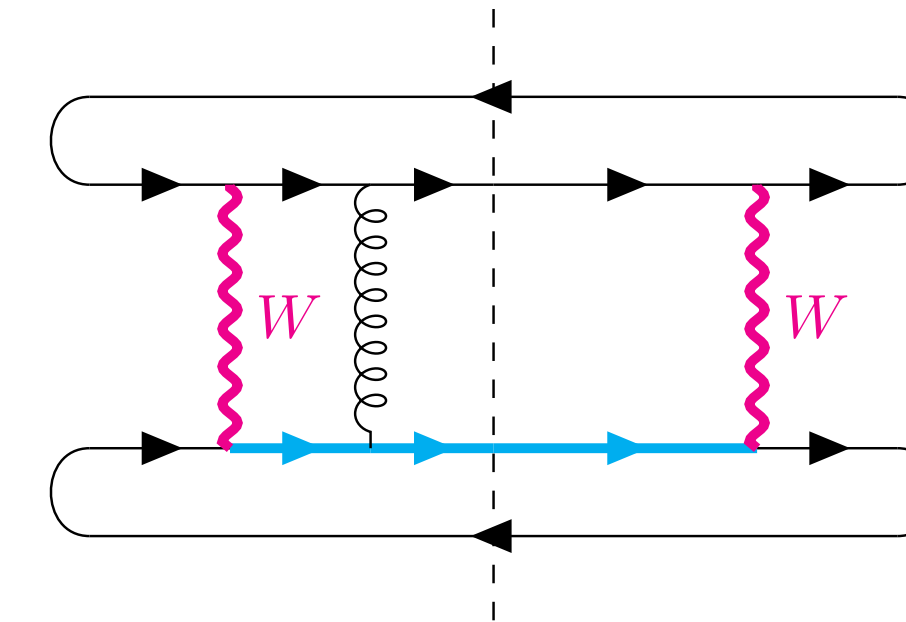
$$\propto \text{Tr}(t^a t^a) = \frac{N_c^2 - 1}{2}$$

NNLO

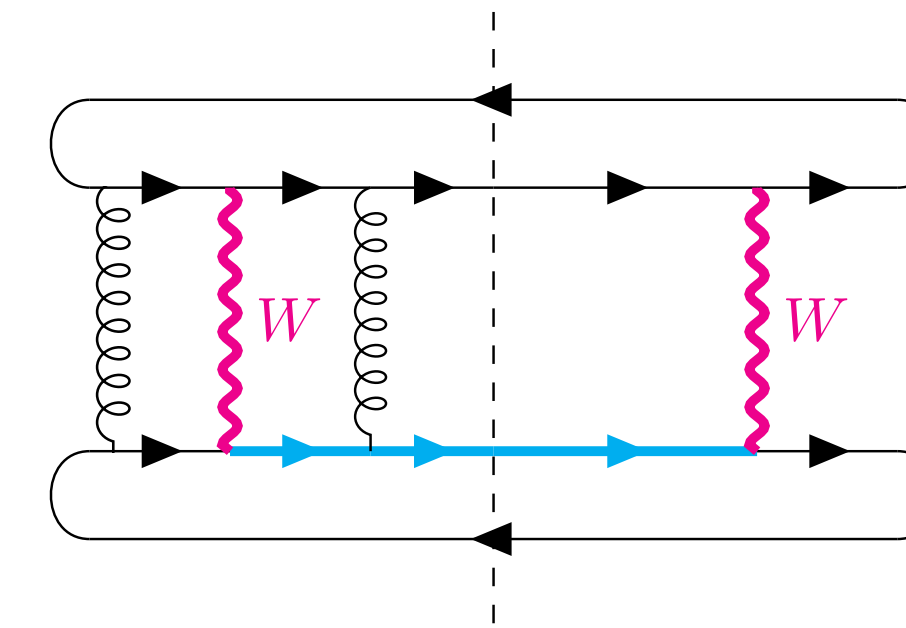


$$\propto \text{Tr}(t^a t^a) \text{Tr}(t^b t^b) = \frac{(N_c^2 - 1)^2}{4}$$

Non-factorisable contributions



$$\propto \text{Tr}(t^a) = 0$$



$$\propto \text{Tr}(t^a t^b) \text{Tr}(t^a t^b) = \frac{N_c^2 - 1}{4}$$

Non-factorisable contributions vanish at NLO due to their colour structure, and are suppressed by a factor $N_c^2 - 1 = 8$ at NNLO.

Non-factorisable corrections: why?

Non-factorisable contributions vanish at NLO due to their colour structure, and are suppressed by a factor $N_c^2 - 1 = 8$ at NNLO.

However:

- Non-factorisable corrections could be enhanced by a factor $\pi^2 \sim 10$ due to the Glauber phase
 - proven for Higgs production in weak boson fusion in the eikonal approximation [Liu, Melnikov et al. '19]
- The actual size of NNLO non-factorisable corrections cannot be inferred from NLO contributions, since they vanish

Even though **non-factorisable contributions** are suppressed by colour it is not guaranteed that they are actually negligible.

In addition:

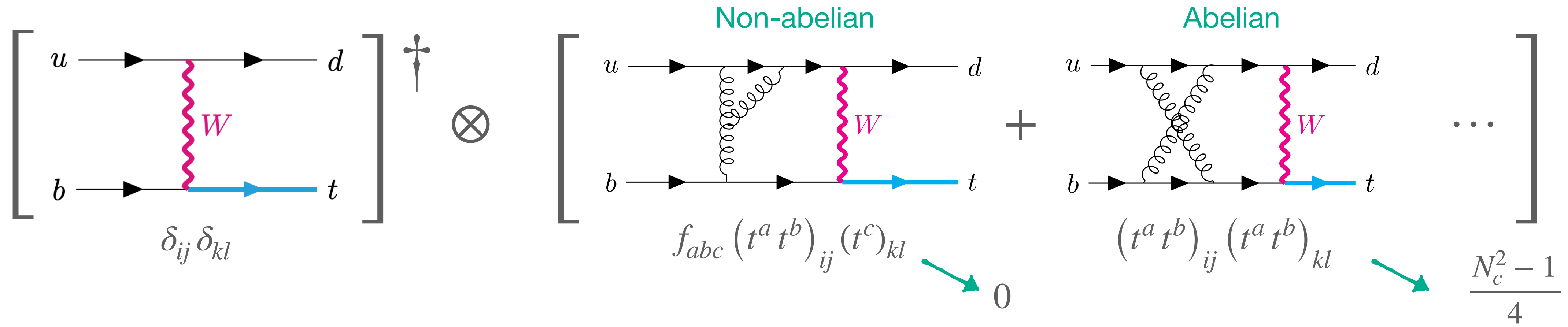
- Inclusive factorisable corrections are very small [Brucherseifer et al. '14] [Berger et al. '16] [Campbell, Neumann et al. '21]

$$\delta\sigma_{\text{fact.}}^{\text{NLO}} \sim (2 - 3\%) \sigma^{\text{LO}}$$

$$\delta\sigma_{\text{fact.}}^{\text{NNLO}} \sim (1 - 3\%) \sigma^{\text{NLO}}$$

Non-factorisable corrections: main properties

Non-factorisable contributions have to **connect upper an lower quark line**, and are effectively **Abelian**



The infrared structure is simplified: **no collinear singularities**

$$\frac{1}{E_g E_q (1 - \cos \theta_{gq})}$$

$$\frac{1}{E_g E_t (1 - \cos \theta_{gt})}$$

All IR singularities are of **soft origin**.

Non-factorisable contributions are **UV finite**

$\delta_{ij} \delta_{kl}$

$(t^a)_{ij} (t^a)_{kl}$

$\alpha_s^{\text{bare}} \mu_0^{2\epsilon} = \alpha_s \mu^{2\epsilon} S_\epsilon$

Renormalisation simply consists of

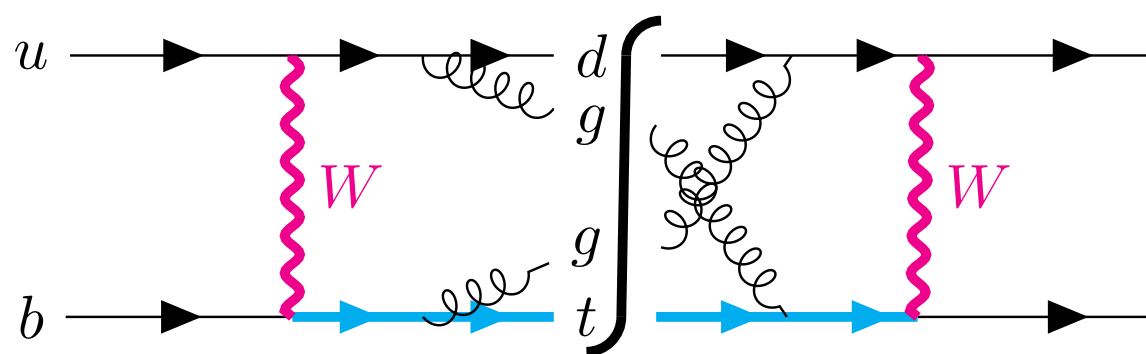
Non-factorisable corrections: ingredients of the calculation

Three terms contribute to the non-factorisable cross section

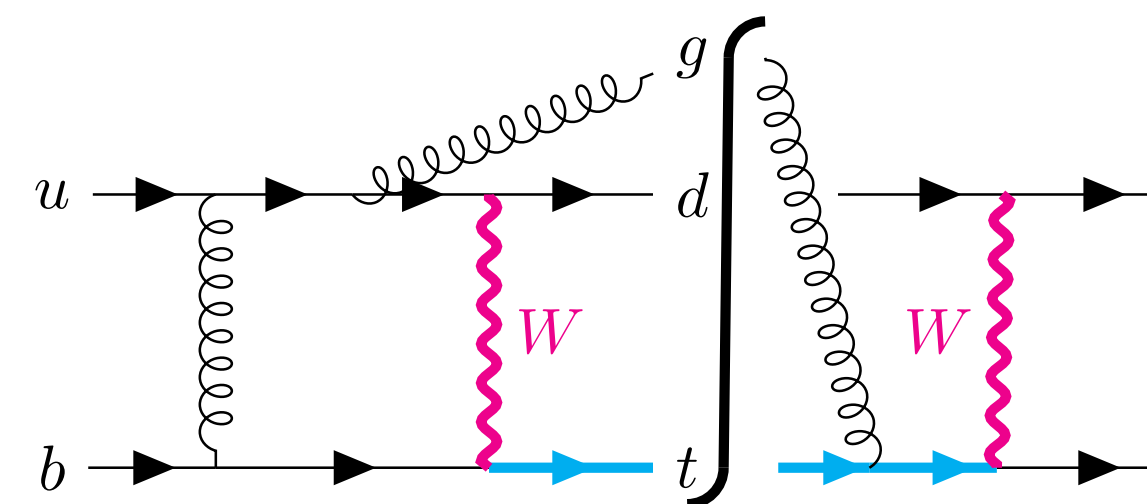
$$d\sigma_{pp \rightarrow X+t}^{\text{nf}} = \sum_{i,j} \int dx_1 dx_2 f_i(x_1, \mu_F) f_j(x_2, \mu_F) d\hat{\sigma}_{ij \rightarrow X+t}^{\text{nf}}(x_1, x_2)$$

$$d\hat{\sigma}_{\text{NNLO}}^{\text{nf}} = d\hat{\sigma}_{\text{RR}}^{\text{nf}} + d\hat{\sigma}_{\text{RV}}^{\text{nf}} + d\hat{\sigma}_{\text{VV}}^{\text{nf}}$$

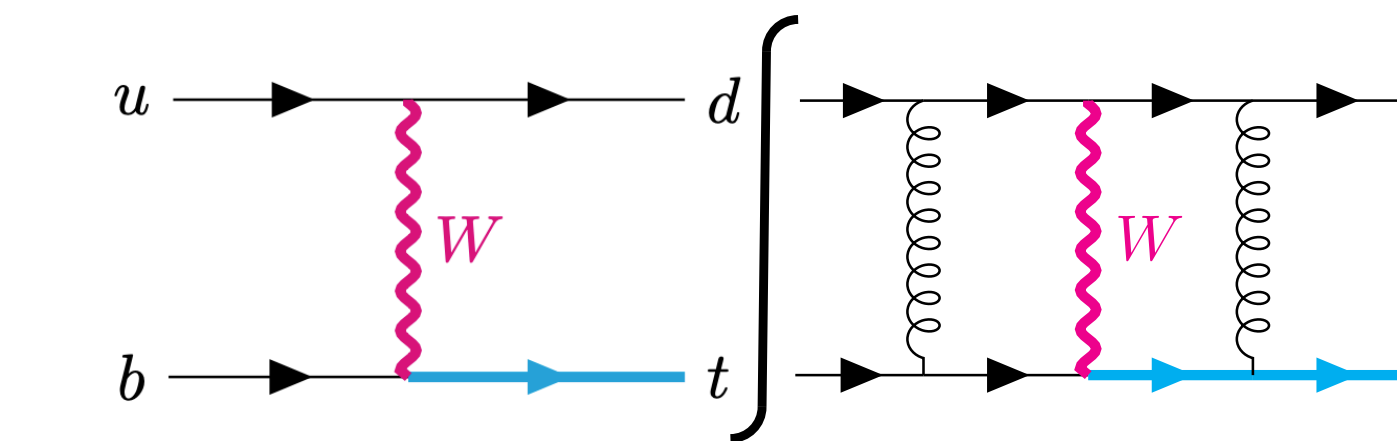
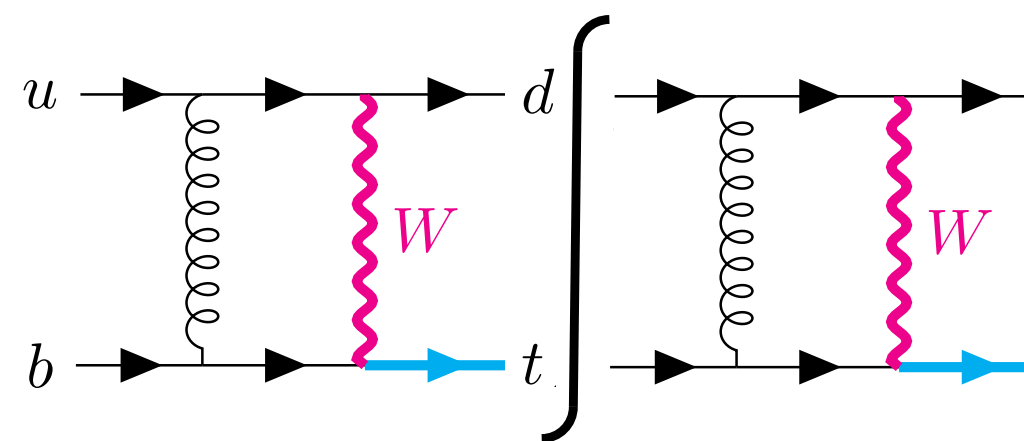
$$d\hat{\sigma}_{\text{RR}}^{\text{nf}} : \mathcal{A}_6^{(0)} \otimes \mathcal{A}_6^{(0)}$$



$$d\hat{\sigma}_{\text{RV}}^{\text{nf}} : \mathcal{A}_5^{(1)} \otimes \mathcal{A}_5^{(0)}$$



$$d\hat{\sigma}_{\text{VV}}^{\text{nf}} : \mathcal{A}_4^{(1)} \otimes \mathcal{A}_4^{(1)}, \mathcal{A}_4^{(0)} \otimes \mathcal{A}_4^{(2)}$$



Each ingredient requires specific treatment and encodes difficulties to overcome

IR singularities

Higher-order corrections are affected by **infrared singularities arising from unresolved radiation**.

- **Virtual corrections:**

- Explicit IR singularities from loop integrations → poles in $1/\epsilon$

- **Real corrections:**

- Singularities after integration over full phase space of radiated parton

$$\text{Diagram: } p \rightarrow p - k \text{ (radiation)} \sim \frac{1}{(p-k)^2} = \frac{1}{2E_p E_k (1 - \cos \theta)} \xrightarrow[E_k \rightarrow 0]{} \infty. \quad \text{or} \quad \theta \rightarrow 0$$

$$\int \frac{d^{d-1}k}{(2\pi)^{d-1} 2E_k} |M(\{p\}, k)|^2 \underset{E_k \rightarrow 0}{\sim} \int \frac{dE_k}{E_k^{1+2\epsilon}} \frac{d\theta}{\theta^{1+2\epsilon}} \times |M(\{p\})|^2 \sim \frac{1}{4\epsilon^2}.$$

- **Integrating implies losing kinematic information** (needed for distributions, kinematic cuts, ...)
- For **non-factorisable** corrections **only soft** limits are relevant → **only $1/\epsilon$ poles**

→ **Subtraction scheme:** extract singularities without integrating over full phase space of radiated partons

$$\int d\Phi_g = \underbrace{\left[\int \text{Diagram: } p \rightarrow p - k \right]}_{\text{Finite in } d=4, \text{ integrable numerically}} - \underbrace{\left[\int \text{Diagram: } p \rightarrow p - k \xrightarrow{E_g \rightarrow 0} \right]}_{\text{exposes the same } 1/\epsilon \text{ poles as the virtual correction}} d\Phi_g + \underbrace{\left[\int \text{Diagram: } p \rightarrow p - k \xrightarrow{E_g \rightarrow 0} \right]}_{\text{exposes the same } 1/\epsilon \text{ poles as the virtual correction}} d\Phi_g$$

Double-real emission

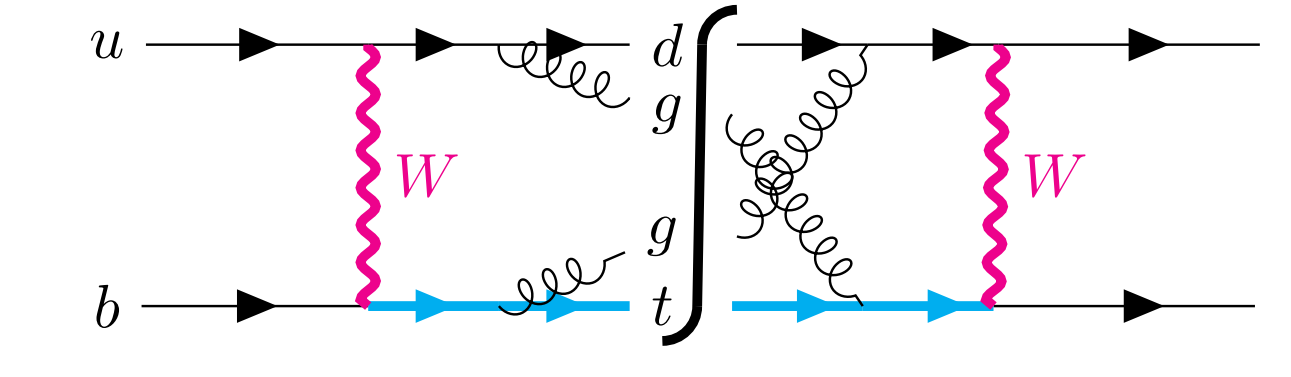
Main issue of the **double-real contribution**: extract and regularise IR singularities preserving the fully-differential nature of the calculation

→ **Nested soft-collinear subtraction scheme** [Caola, Melnikov, Röntsch 1702.01352]

$$F_{\text{LM}}^{\text{nf}}(1_q, 2_b, 3_{q'}, 4_t; 5_g, 6_g) = \mathcal{N} \int d\text{Lips}_{34} (2\pi)^d \delta^{(d)}(p_1 + p_2 - \sum_{i=3}^6 p_i) \times | \mathcal{A}_0(1_q, 2_b, 3_{q'}, 4_t; 5_g, 6_g) |_{\text{nf}}^2$$

Integration over potentially unresolved phase space

$$[dp] = \frac{d^{d-1}p}{(2\pi)^{d-1} 2E_p} \theta(E_{\max} - E_p)$$



Separate the **soft-divergent part** from the **soft-finite contribution**

$$\langle F_{\text{LM}}^{\text{nf}}(1_q, 2_b, 3_{q'}, 4_t; 5_g, 6_g) \rangle = \langle S_5 S_6 F_{\text{LM}}^{\text{nf}}(1_q, 2_b, 3_{q'}, 4_t; 5_g, 6_g) \rangle$$



Double-soft counterterm

$$+ 2 \langle S_6 (I - S_5) F_{\text{LM}}^{\text{nf}}(1_q, 2_b, 3_{q'}, 4_t; 5_g, 6_g) \rangle$$



Single-soft counterterm

$$+ \langle (I - S_5) (I - S_6) F_{\text{LM}}^{\text{nf}}(1_q, 2_b, 3_{q'}, 4_t; 5_g, 6_g) \rangle$$



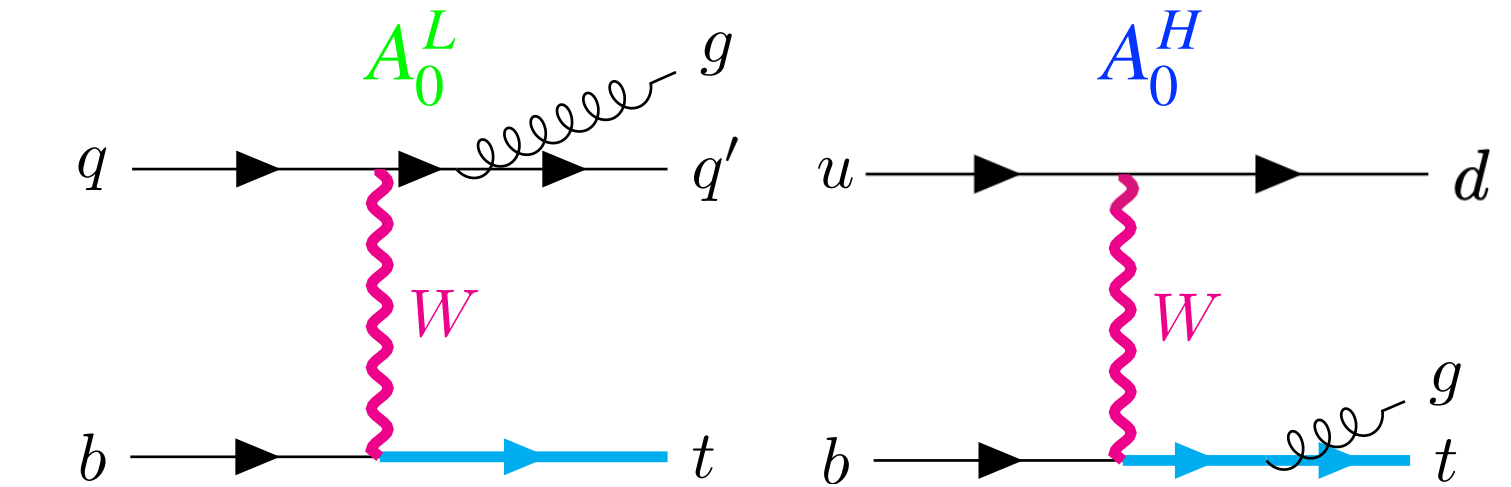
Resolved contribution

Dealing with soft limits

Consider **single emission**: simpler bookkeeping, clear procedure

1. Decompose the amplitude into **colour-stripped, sub-amplitudes**

$$\langle c | \mathcal{A}_0(1_q, 2_b, 3_{q'}, 4_t; 5_g) \rangle = g_{s,b} \left[t_{c_3 c_1}^{c_5} \delta_{c_4 c_2} A_0^L(5_g) + t_{c_4 c_2}^{c_5} \delta_{c_3 c_1} A_0^H(5_g) \right]$$



2. Under **soft limit**, sub-amplitudes factorise into **universal eikonal factors** and **lower-multiplicity amplitudes**

$$S_5 \quad A_0^{L/H}(5_g) = \varepsilon_\mu^{(\lambda)}(5) \ J^\mu(3,1;5) \ A_0(1_q, 2_b, 3_{q'}, 4_t)$$

$$J^\mu(i,j;k) = \frac{p_i^\mu}{p_i \cdot p_k} - \frac{p_j^\mu}{p_j \cdot p_k}$$

3. **Contract sub-amplitudes** to connect different quark lines

$$S_5 \ 2\text{Re} [A_0^L(5_g) A_0^{H*}(5_g)] = \sum_\lambda \varepsilon_\mu^{(\lambda)*}(5) \varepsilon_\nu^{(\lambda)}(5) \ J^\mu(3,1;5) \ J^\nu(4,2;5) \ |A_0(1_q, 2_b, 3_{q'}, 4_t)|^2$$

$$= - \boxed{\text{Eik}_{\text{nf}}(1_q, 2_b, 3_{q'}, 4_t; 5_g)} \ |A_0(1_q, 2_b, 3_{q'}, 4_t)|^2$$

$$\text{Eik}_{\text{nf}}(1_q, 2_b, 3_{q'}, 4_t; k_g) = J^\mu(3,1;k) J_\mu(4,2;k) = \sum_{\substack{i \in [1,3] \\ j \in [2,4]}} \frac{\lambda_{ij} \ p_i \cdot p_j}{(p_i \cdot p_k)(p_j \cdot p_k)}$$

Dealing with soft limits

- Integrate the eikonal factor over the radiation phase space

$$g_{s,b}^2 \int [dp_k] \text{Eik}_{\text{nf}}(1_q, 2_b, 3_{q'}, 4_t; k_g) \equiv \frac{\alpha_s}{2\pi} \left(\frac{2E_{\max}}{\mu} \right)^{-2\epsilon} K_{\text{nf}}(1_q, 2_b, 3_{q'}, 4_t; \epsilon) = \frac{\alpha_s}{2\pi} \left(\frac{2E_{\max}}{\mu} \right)^{-2\epsilon} \left[\frac{1}{\epsilon} \log \left(\frac{p_1 \cdot p_4}{p_1 \cdot p_2} \frac{p_2 \cdot p_3}{p_3 \cdot p_4} \right) + \mathcal{O}(\epsilon^0) \right]$$

Double-real correction treated in the same fashion:

- Independent emissions
- Factorised double-soft limit

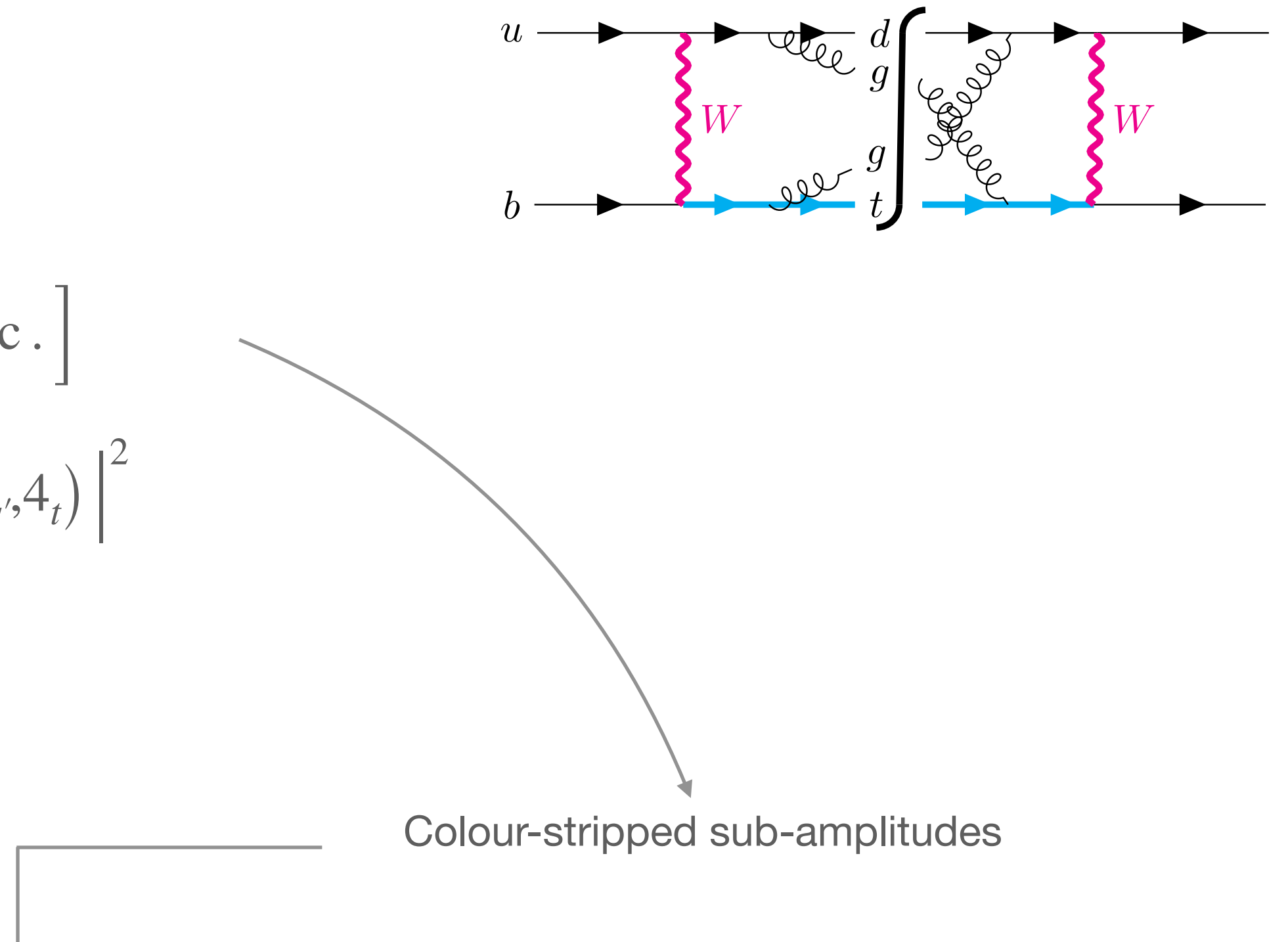
$$S_6 \left| \mathcal{A}_0(1_q, 2_b, 3_{q'}, 4_t; 5_g, 6_g) \right|_{\text{nf}}^2 = - g_{s,b}^4 \frac{N^2 - 1}{2} \text{Eik}_{\text{nf}}(6_g) \left[A_0^L(5_g) A_0^{H*}(5_g) + \text{c.c.} \right]$$

$$S_5 S_6 \left| \mathcal{A}_0(1_q, 2_b, 3_{q'}, 4_t; 5_g, 6_g) \right|_{\text{nf}}^2 = g_{s,b}^4 (N^2 - 1) \text{Eik}_{\text{nf}}(5_g) \text{Eik}_{\text{nf}}(6_g) \left| A_0(1_q, 2_b, 3_{q'}, 4_t) \right|^2$$

Double-real at cross-section level results in a remarkably simple object

$$2s \cdot \sigma_{RR} = \left(\frac{\alpha_s}{2\pi} \right)^2 \frac{N^2 - 1}{2N^2} \left(\frac{2E_{\max}}{\mu} \right)^{-4\epsilon} \langle K_{\text{nf}}^2(\epsilon) F_{\text{LM}}(1_q, 2_b, 3_{q'}, 4_t) \rangle$$

$$- \left(\frac{\alpha_s}{2\pi} \right) \frac{N^2 - 1}{2} \left(\frac{2E_{\max}}{\mu} \right)^{-2\epsilon} \langle K_{\text{nf}}(\epsilon) (I - S_5) \widetilde{F}_{\text{LM}}^{\text{nf}}(1_q, 2_b, 3_{q'}, 4_t; 5_g) \rangle + \langle (I - S_5)(I - S_6) F_{\text{LM}}^{\text{nf}}(1_q, 2_b, 3_{q'}, 4_t; 5_g, 6_g) \rangle$$

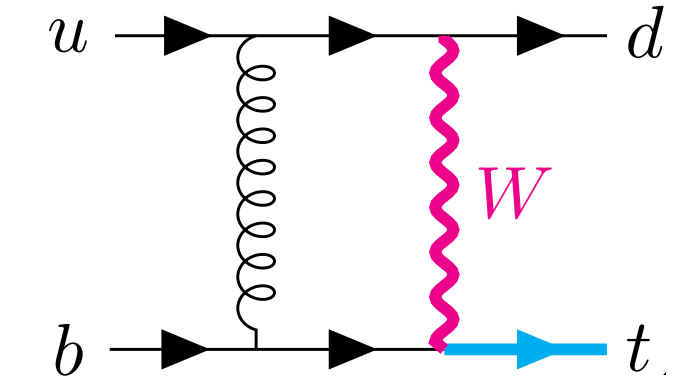


Double-virtual contribution

Extract IR singularities from virtual radiation and compute finite contributions.

1. One-loop correction to the 4-point amplitude

$$\langle c | \mathcal{A}_1(1_q, 2_b, 3_{q'}, 4_t) \rangle = \frac{\alpha_s}{2\pi} \left(\dots + t_{c_3 c_1}^a t_{c_4 c_2}^a B_1(1_q, 2_b, 3_{q'}, 4_t) \right)$$



B_1 is UV-finite, but IR-divergent: the abelian nature of the correction leads to the simple pole structure

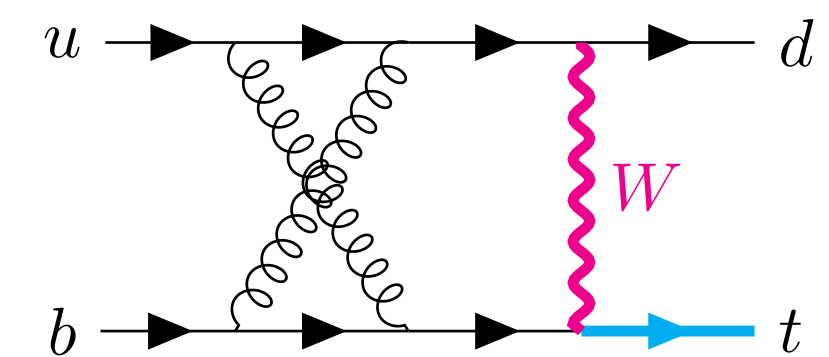
$$B_1(1_q, 2_b, 3_{q'}, 4_t) = \textcolor{red}{I}_1(\epsilon) A_0(1_q, 2_b, 3_{q'}, 4_t) + \textcolor{blue}{B}_{1,\text{fin}}(1_q, 2_b, 3_{q'}, 4_t)$$

$$I_1(\epsilon) \equiv I_1(1_q, 2_b, 3_{q'}, 4_t; \epsilon) = \frac{1}{\epsilon} \left[\log \left(\frac{p_1 \cdot p_4 \ p_2 \cdot p_3}{p_1 \cdot p_2 \ p_3 \cdot p_4} \right) + 2\pi i \right]$$

2. Two-loop correction to the 4-point amplitude

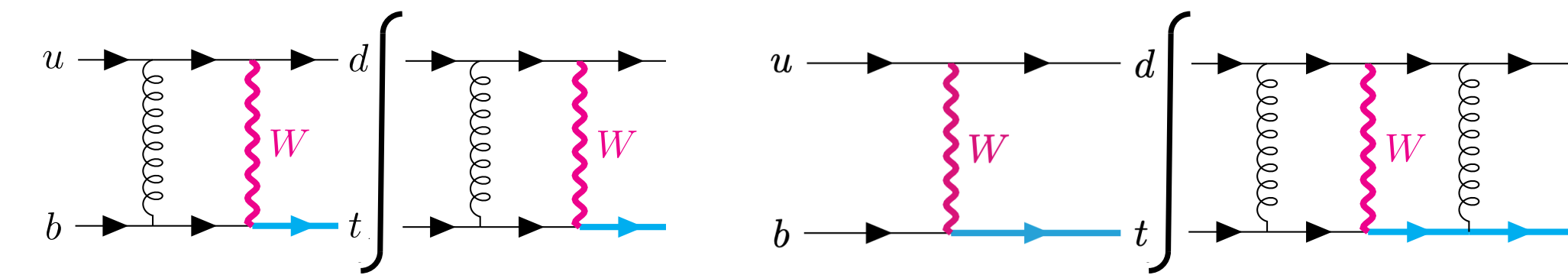
$$\langle c | \mathcal{A}_2(1_q, 2_b, 3_{q'}, 4_t) \rangle = \left(\frac{\alpha_s}{2\pi} \right)^2 \left(\dots + \frac{1}{2} \{t^a, t^b\}_{c_3 c_1} \frac{1}{2} \{t^a, t^b\}_{c_4 c_2} B_2(1_q, 2_b, 3_{q'}, 4_t) \right)$$

$$B_2(1_q, 2_b, 3_{q'}, 4_t) = -\frac{\textcolor{red}{I}_1^2(\epsilon)}{2} A_0(1_q, 2_b, 3_{q'}, 4_t) + \textcolor{red}{I}_1(\epsilon) B_1(1_q, 2_b, 3_{q'}, 4_t) + \textcolor{blue}{B}_{2,\text{fin}}(1_q, 2_b, 3_{q'}, 4_t)$$



Double-virtual contribution

Complete double-virtual cross section cast in a very compact expression



$$2s \cdot \sigma_{\text{VV}} = \langle F_{\text{LVV}}^{\text{nf}}(1_q, 2_b, 3_{q'}, 4_t) \rangle = \left(\frac{\alpha_s}{2\pi} \right)^2 \frac{N^2 - 1}{4} \left[\frac{2}{N^2} \left\langle (\text{Re} [I_1(\epsilon)])^2 F_{\text{LM}}(1_q, 2_b, 3_{q'}, 4_t) \right\rangle \right.$$

$$\left. + 2 \left\langle \text{Re} [I_1(\epsilon)] \widetilde{F}_{\text{LV,fin}}^{\text{nf}}(1_q, 2_b, 3_{q'}, 4_t) \right\rangle + \left\langle \widetilde{F}_{\text{VV,fin}}^{\text{nf}}(1_q, 2_b, 3_{q'}, 4_t) \right\rangle \right]$$

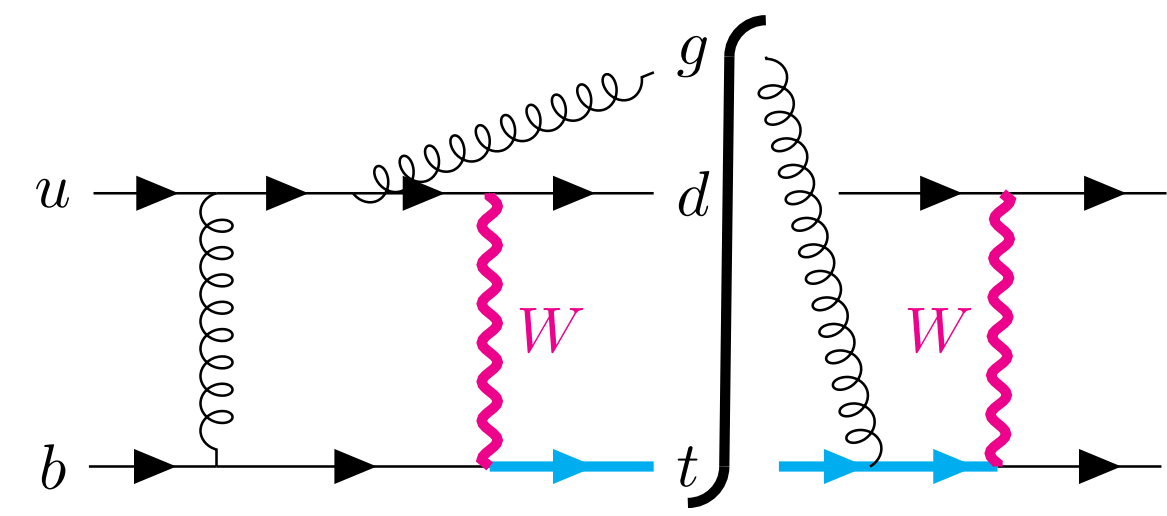
Finite contributions built on one- and two-loop color stripped amplitudes

$$\widetilde{F}_{\text{LV,fin}}^{\text{nf}}(1_q, 2_b, 3_{q'}, 4_t) = \mathcal{N} \int d\text{Lips}_{34} (2\pi)^d \delta^{(d)}(p_1 + p_2 - p_3 - p_4) 2\text{Re} \left[A_0^*(1_q, 2_b, 3_{q'}, 4_t) \mathbf{B}_{1,\text{fin}}(1_q, 2_b, 3_{q'}, 4_t) \right]$$

$$\widetilde{F}_{\text{VV,fin}}^{\text{nf}}(1_q, 2_b, 3_{q'}, 4_t) = \mathcal{N} \int d\text{Lips}_{34} (2\pi)^d \delta^{(d)}(p_1 + p_2 - p_3 - p_4) \left\{ \left| \mathbf{B}_{1,\text{fin}}(1_q, 2_b, 3_{q'}, 4_t) \right|^2 + 2\text{Re} \left[A_0^*(1_q, 2_b, 3_{q'}, 4_t) \mathbf{B}_{2,\text{fin}}(1_q, 2_b, 3_{q'}, 4_t) \right] \right\}$$

Real-virtual contribution

Extract IR singularities both from **real and virtual radiation**



$$F_{\text{LV}}^{\text{nf}}(1_q, 2_b, 3_{q'}, 4_t; 5_g) = \mathcal{N} \int d\text{Lips}_{34} (2\pi)^d \delta^{(d)} \left(p_1 + p_2 - \sum_{i=3}^5 p_i \right) 2\text{Re} \left[\mathcal{A}_0^*(1_q, 2_b, 3_{q'}, 4_t; 5_g) \mathcal{A}_1(1_q, 2_b, 3_{q'}, 4_t; 5_g) \right]_{\text{nf}}$$

1. First extract phase-space singularities

$$2s \cdot \sigma_{\text{RV}} = \int [dp_5] F_{\text{LV}}^{\text{nf}}(1_q, 2_b, 3_{q'}, 4_t; 5_g) = \langle S_5 F_{\text{LV}}^{\text{nf}}(1_q, 2_b, 3_{q'}, 4_t; 5_g) \rangle_{\text{Soft-divergent}} + \langle (I - S_5) F_{\text{LV}}^{\text{nf}}(1_q, 2_b, 3_{q'}, 4_t; 5_g) \rangle_{\text{Soft-regulated}}$$

2. Notice that **both contributions** contain explicit poles in ϵ

IR divergencies of one-loop amplitudes do **not depend on the real radiation** \rightarrow same $I_1(\epsilon)$ as VV

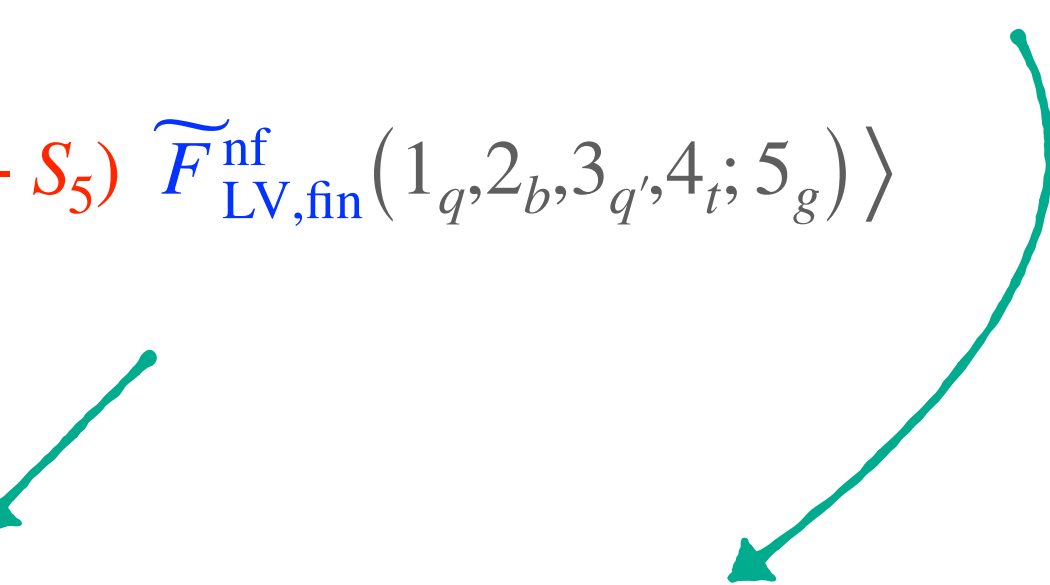
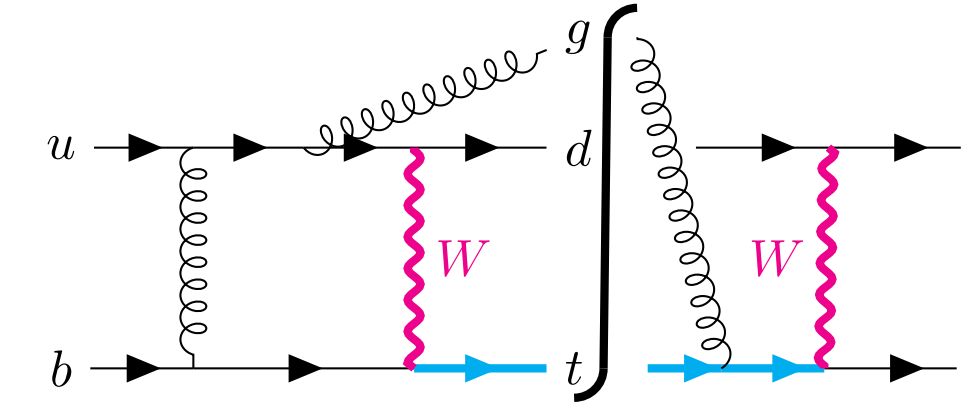
Real radiation in the **soft limit** exposes the usual eikonal factor \rightarrow same $\text{Eik}_{\text{nf}}(k_g)$ as RR

Real-virtual contribution

Complete double-virtual cross section cast in a very compact expression

$$2s \cdot \sigma_{\text{RV}} = \int [dp_5] F_{\text{LV}}^{\text{nf}}(1_q, 2_b, 3_{q'}, 4_t; 5_g) = \langle S_5 F_{\text{LV}}^{\text{nf}}(1_q, 2_b, 3_{q'}, 4_t; 5_g) \rangle + \langle (I - S_5) F_{\text{LV}}^{\text{nf}}(1_q, 2_b, 3_{q'}, 4_t; 5_g) \rangle$$

$$\begin{aligned} \langle S_5 F_{\text{LV}}^{\text{nf}}(1_q, 2_b, 3_{q'}, 4_t; 5_g) \rangle &= -\left(\frac{\alpha_s}{2\pi}\right)^2 \frac{N^2 - 1}{N^2} \left(\frac{2E_{\max}}{\mu}\right)^{-2\epsilon} \langle K_{\text{nf}}(\epsilon) \text{Re}[I_1(\epsilon)] F_{\text{LM}}(1_q, 2_b, 3_{q'}, 4_t) \rangle - \left(\frac{\alpha_s}{2\pi}\right)^2 \frac{N^2 - 1}{2} \left(\frac{2E_{\max}}{\mu}\right)^{-2\epsilon} \langle K_{\text{nf}}(\epsilon) \widetilde{F}_{\text{LV,fin}}^{\text{nf}}(1_q, 2_b, 3_{q'}, 4_t) \rangle \\ \langle (I - S_5) F_{\text{LV}}^{\text{nf}}(1_q, 2_b, 3_{q'}, 4_t; 5_g) \rangle &= \left(\frac{\alpha_s}{2\pi}\right) \frac{N^2 - 1}{2} \langle \text{Re}[I_1(\epsilon)] (I - S_5) \widetilde{F}_{\text{LM}}^{\text{nf}}(1_q, 2_b, 3_{q'}, 4_t; 5_g) \rangle + \left(\frac{\alpha_s}{2\pi}\right) \frac{N^2 - 1}{4} \langle (I - S_5) \widetilde{F}_{\text{LV,fin}}^{\text{nf}}(1_q, 2_b, 3_{q'}, 4_t; 5_g) \rangle \end{aligned}$$



Finite contributions built on one-loop, 4-point and 5-point color stripped amplitudes

$$\widetilde{F}_{\text{LV,fin}}^{\text{nf}}(1_q, 2_b, 3_{q'}, 4_t) = \mathcal{N} \int d\text{Lips}_{34} (2\pi)^d \delta^{(d)}(p_1 + p_2 - p_3 - p_4) 2\text{Re} \left[A_0^*(1_q, 2_b, 3_{q'}, 4_t) B_{1,\text{fin}}(1_q, 2_b, 3_{q'}, 4_t) \right]$$

$$\widetilde{F}_{\text{LV,fin}}^{\text{nf}}(1_q, 2_b, 3_{q'}, 4_t; 5_g) = \mathcal{N} \int d\text{Lips}_{34} (2\pi)^d \delta^{(d)}(p_1 + p_2 - \sum_{i=3}^5 p_i) g_{s,b}^2 \left(A_0^{L*}(5_g) B_{1,\text{fin}}^{sH}(5_g) + A_0^{H*}(5_g) B_{1,\text{fin}}^{sL}(5_g) + \text{c.c.} \right)$$

Pole cancellation

Manifestly finite result: combination of RR, VV and RV → split into contributions of **different multiplicities**

$$\sigma_{\text{nf}} = \sigma_{\text{nf}}^{(2g)} + \sigma_{\text{nf}}^{(1g)} + \sigma_{\text{nf}}^{(0g)}$$

$\sigma_{\text{nf}}^{(2g)}$: **fully resolved**, implemented numerically

$\sigma_{\text{nf}}^{(1g), (0g)}$: finite due to **cancellation of real and virtual singularities**

$$\mathcal{W}(1_q, 2_b, 3_{q'}, 4_t) = \left(\frac{2E_{\max}}{\mu} \right)^{-2\epsilon} K_{\text{nf}}(\epsilon) - \text{Re}[I_1(\epsilon)] = \mathcal{O}(\epsilon^0)$$

$$2s \cdot \sigma_{\text{nf}}^{(1g)} = - \left(\frac{\alpha_s}{2\pi} \right) \frac{N^2 - 1}{2} \langle \mathcal{W}(1_q, 2_b, 3_{q'}, 4_t) (I - S_5) \widetilde{F}_{\text{LM}}^{\text{nf}}(1_q, 2_b, 3_{q'}, 4_t; 5_g) \rangle + \left(\frac{\alpha_s}{2\pi} \right) \frac{N^2 - 1}{4} \langle (I - S_5) \widetilde{F}_{\text{LV,fin}}^{\text{nf}}(1_q, 2_b, 3_{q'}, 4_t; 5_g) \rangle$$

$$2s \cdot \sigma_{\text{nf}}^{(0g)} = \left(\frac{\alpha_s}{2\pi} \right)^2 \frac{N^2 - 1}{2N^2} \langle \mathcal{W}^2(1_q, 2_b, 3_{q'}, 4_t) F_{\text{LM}}(1_q, 2_b, 3_{q'}, 4_t) \rangle - \left(\frac{\alpha_s}{2\pi} \right)^2 \frac{N^2 - 1}{2} \langle \mathcal{W}(1_q, 2_b, 3_{q'}, 4_t) \widetilde{F}_{\text{LV,fin}}^{\text{nf}}(1_q, 2_b, 3_{q'}, 4_t) \rangle + \left(\frac{\alpha_s}{2\pi} \right)^2 \frac{N^2 - 1}{4} \langle \widetilde{F}_{\text{VV,fin}}^{\text{nf}}(1_q, 2_b, 3_{q'}, 4_t) \rangle$$

In the entire procedure the only amplitude which must be expanded to $\mathcal{O}(\epsilon)$ is $B_1(1_q, 2_b, 3_{q'}, 4_t)$ as it is needed to extract the two-loop finite remainder $B_{2,\text{fin}}(1_q, 2_b, 3_{q'}, 4_t)$.

Amplitude evaluation

Diagrams generated with QGRAPH and processed with FORM.

W boson forces **light quark** to be **left-handed** and we decompose the **massive momentum** into **2 massless momenta**

$$p_4 = p_4^\flat + \frac{m_t^2}{2n \cdot p_4} n$$

$$\bar{u}_L(p_4) = \langle 4^\flat | + \frac{m_t}{[n4^\flat]} [n] \quad , \quad \bar{u}_R(p_4) = [4^\flat | + \frac{m_t}{\langle n4^\flat \rangle} \langle n |$$

The auxiliary momentum n can be appropriately chosen to simplify the result

RV: one-loop five-point amplitude

- 24 diagrams: 8 pentagons and 16 boxes
- 7 kinematic scales

VV: two-loop four-point amplitude [\[Brønnum-Hansen, Melnikov, Quarroz, Wang '21\]](#)

- 18 diagrams: all topologies maximal
- 4 kinematic scales: s, t, m_t^2, m_W^2
- 428 master integrals evaluated numerically using the auxiliary mass flow method to 20 digits in ~ 30 min on a single core
- 10 sets of 10^4 points extracted from a grid prepared on the Born squared amplitude

Amplitude evaluation

Diagrams generated with QGRAPH and processed with FORM.

W boson forces **light quark to be left-handed** and we decompose the **massive momentum into 2 massless momenta**

$$p_4 = p_4^\flat + \frac{m_t^2}{2n \cdot p_4} n$$

$$\bar{u}_L(p_4) = \langle 4^\flat | + \frac{m_t}{[n4^\flat]} [n] \quad , \quad \bar{u}_R(p_4) = [4^\flat | + \frac{m_t}{\langle n4^\flat \rangle} \langle n |$$

The auxiliary momentum n can be appropriately chosen to simplify the result

RV: one-loop five-point amplitude

- 24 diagrams: 8 pentagons and 16 boxes
- 7 kinematic scales

VV: two-loop four-point amplitude [\[Brønnum-Hansen, Melnikov, Quarroz, Wang '21\]](#)

- 18 diagrams: all topologies maximal

	ϵ^{-2}	ϵ^{-1}
$\langle \mathcal{A}^{(0)} \mathcal{A}_{\text{nf}}^{(2)} \rangle$ IR poles	$-229.0940408654660 - 8.978163333241640i$ $-229.0940408654665 - 8.978163333241973i$	$-301.1802988944764 - 264.1773596529505i$ $-301.1802988944791 - 264.1773596529535i$

Results

Differential cross section:

pp collision: $\sqrt{s} = 13\text{TeV}$, PDFs: CT14_lo@LO, CT14_nnlo@NNLO, $m_W = 80.379\text{GeV}$, $m_t = 173.0\text{GeV}$, $\alpha_s(m_t) = 0.108$, $\mu_F = m_t$.

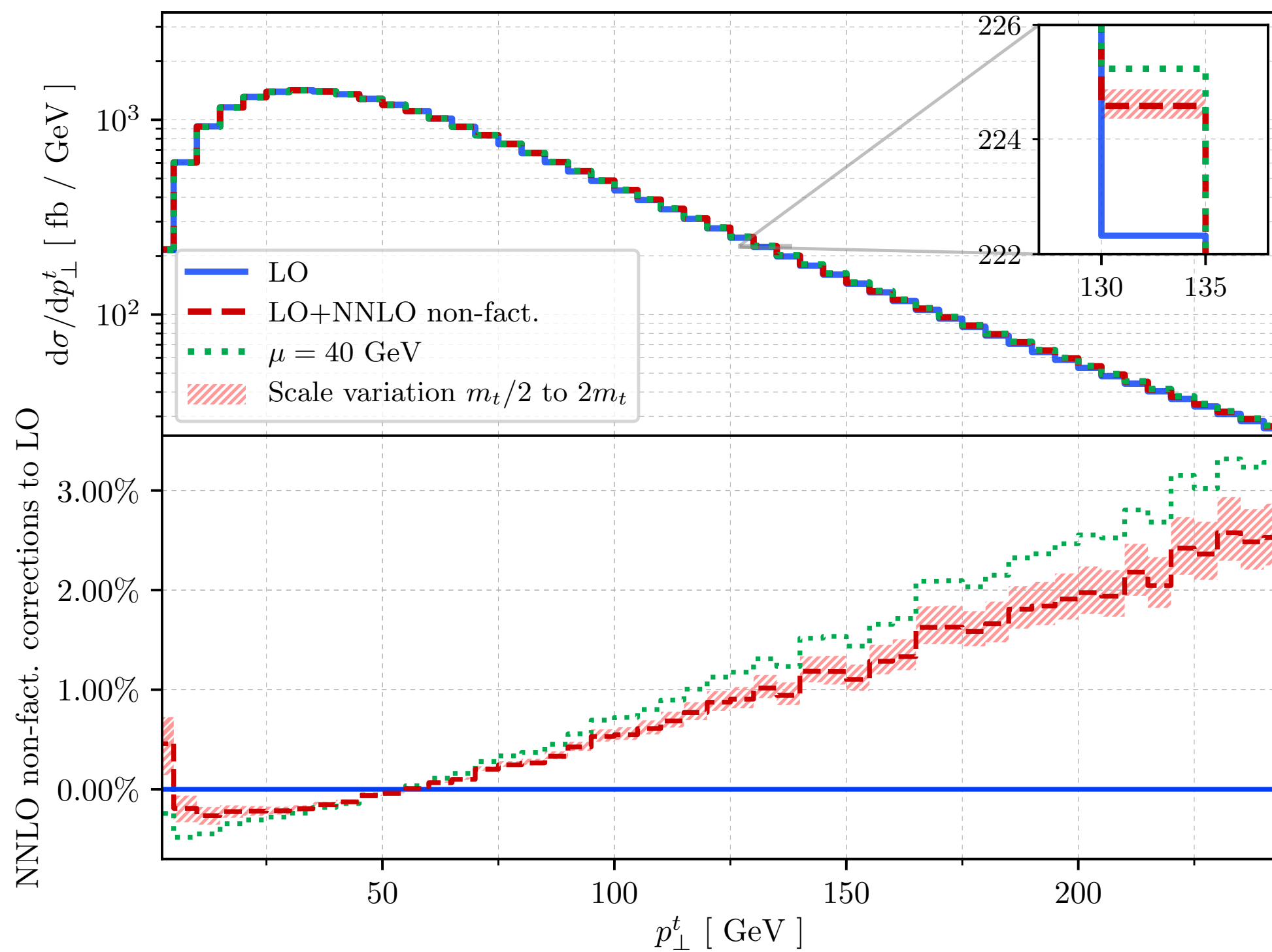
$$\frac{\sigma_{pp \rightarrow X+t}}{1 \text{ pb}} = 117.96 + 0.26 \left(\frac{\alpha_s(\mu_R)}{0.108} \right)^2$$

1. Non-factorisable corrections are $0.22^{-0.04}_{+0.05}\%$ LO for $\mu_R = m_t$.
2. **Theoretical uncertainties** are estimated through **scale variation**: $2m_t, m_t/2$.
3. **Unclear optimal scale choice**: non-factorisable corrections appear for the first time at NNLO \rightarrow no indication from lower orders.
4. For $\mu_R = 40\text{GeV}$ (typical **transfer momentum scale** of top quark) non-factorisable corrections are 0.35% LO.
5. In comparison, **NNLO factorisable** corrections to **NLO cross section** are around 0.7% .

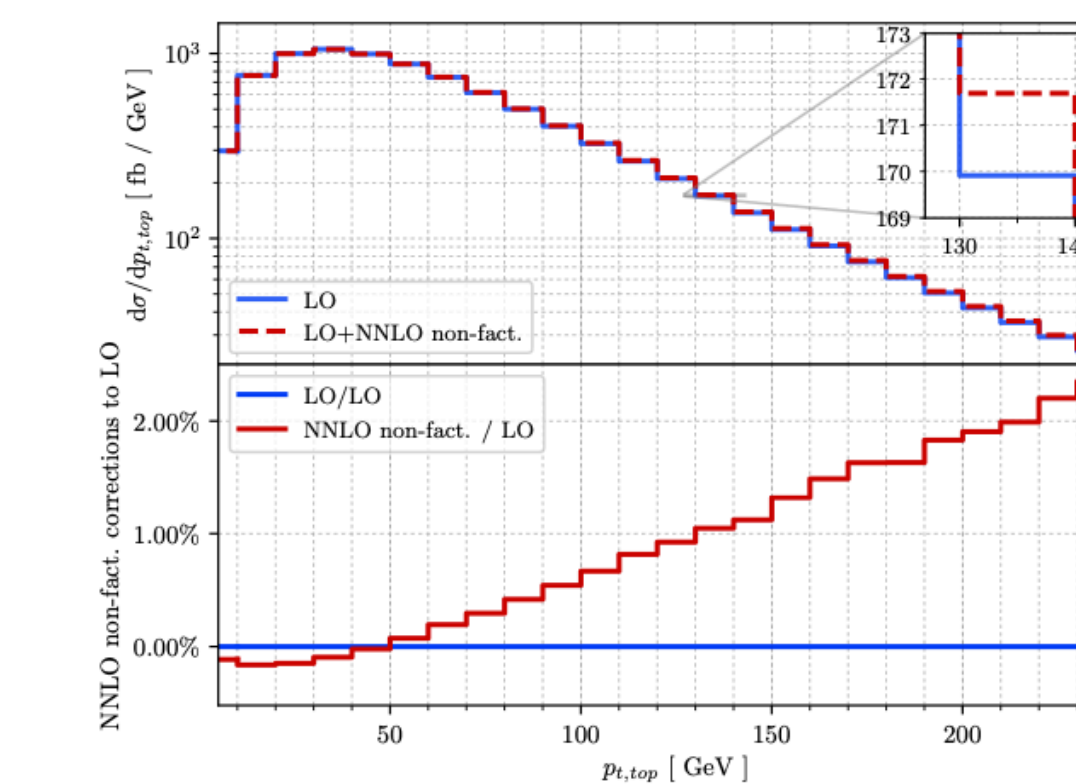
Results

Differential cross section:

pp collision: $\sqrt{s} = 13\text{TeV}$, PDFs: CT14_lo@LO, CT14_nnlo@NNLO, $m_W = 80.379\text{GeV}$, $m_t = 173.0\text{GeV}$, $\alpha_s(m_t) = 0.108$.



1. Non-factorisable corrections are p_{\perp}^t -dependent.
2. Non-factorisable corrections are small and negative at low values of p_{\perp}^t . They vanish at $p_{\perp}^t \sim 50\text{GeV}$ [in agreement with results for virtual corrections]



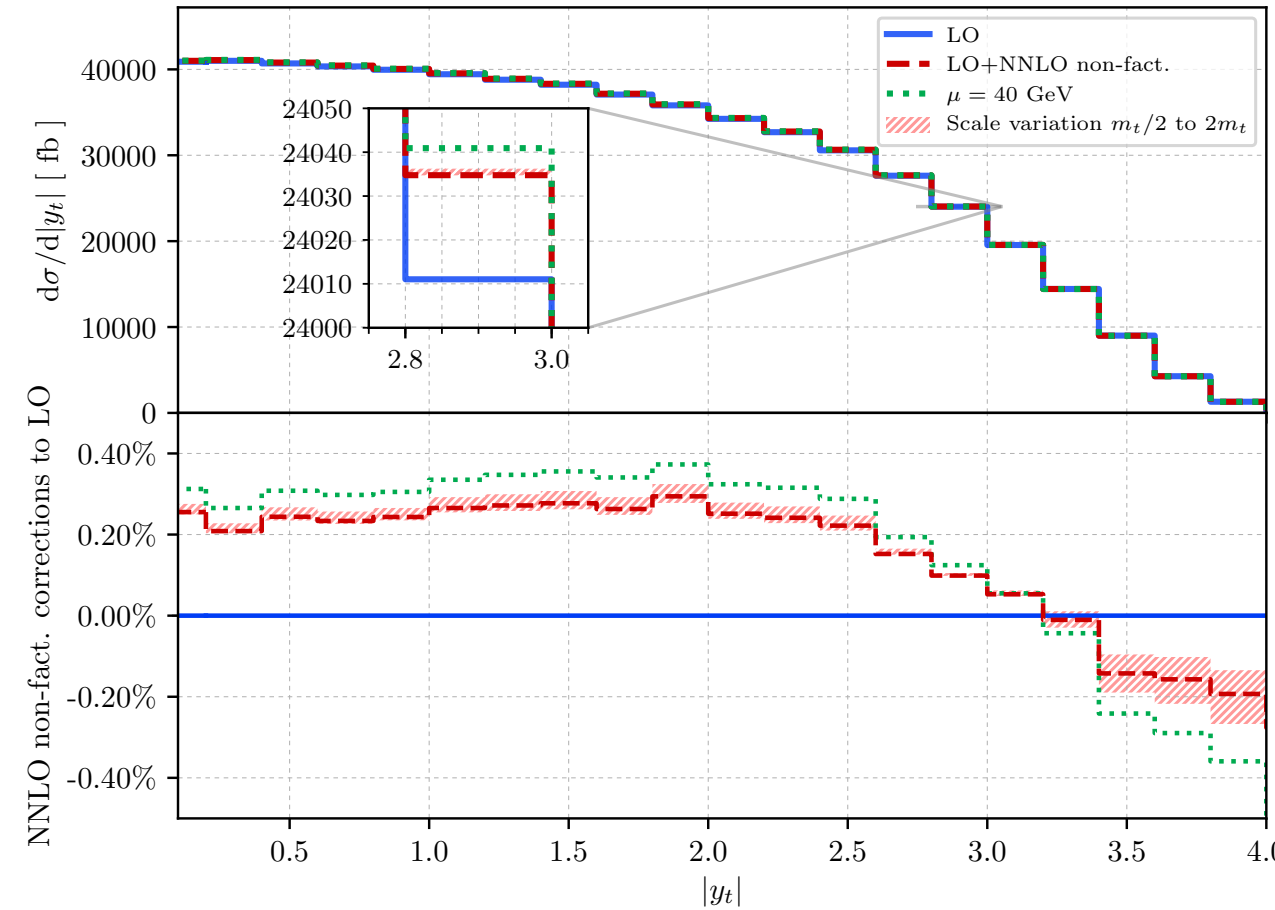
[Brønnum-Hansen,
Melnikov, Quarroz,
Wang '21]

3. Factorisable corrections vanish around $p_{\perp}^t \sim 30\text{GeV}$.
4. Factorisable and non-factorisable corrections are comparable in the region around the maximum of the p_{\perp}^t distribution.

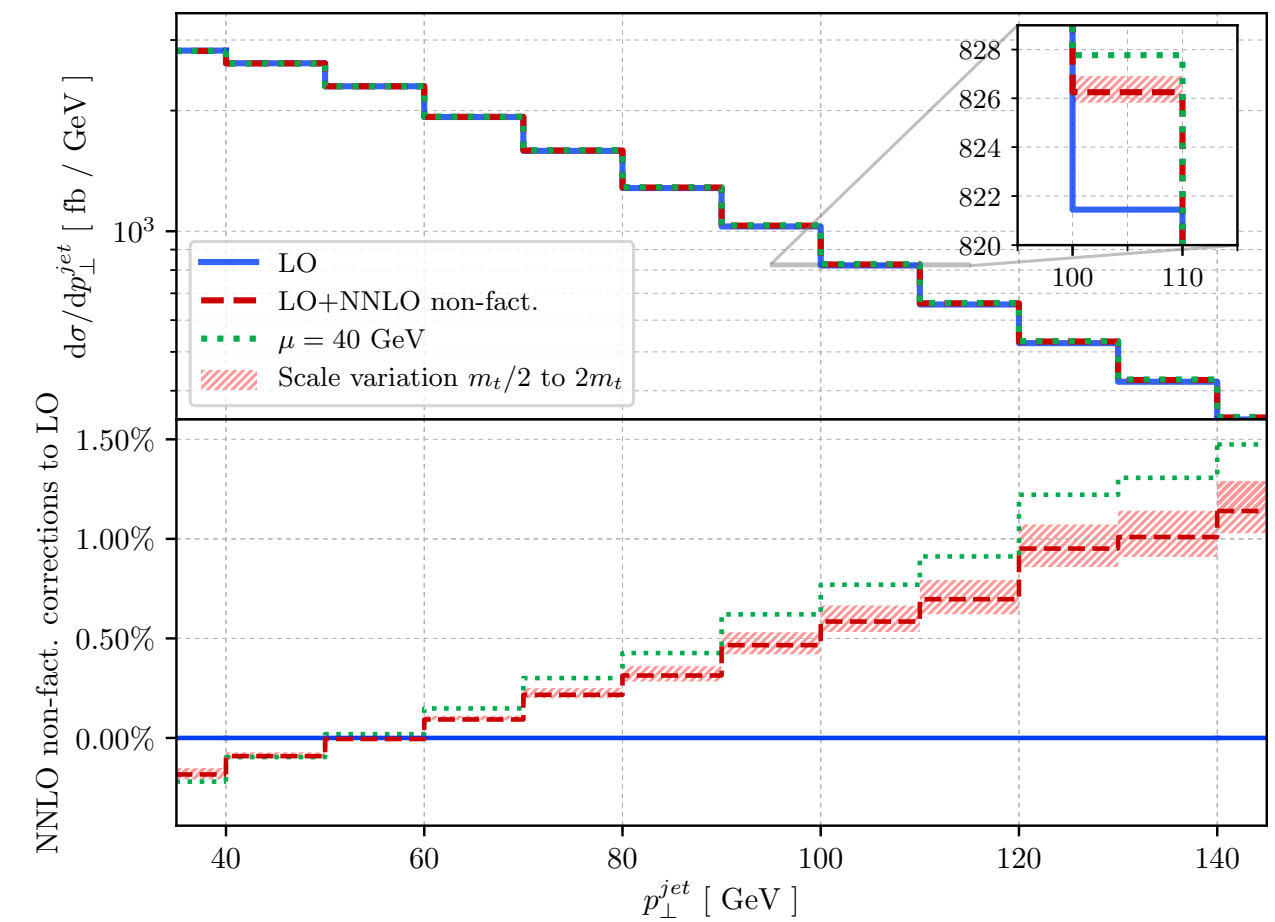
Results

Differential cross section:

pp collision: $\sqrt{s} = 13\text{TeV}$, PDFs: CT14_lo@LO, CT14_nnlo@NNLO, $m_W = 80.379\text{GeV}$, $m_t = 173.0\text{GeV}$, $\alpha_s(m_t) = 0.108$.



1. Relative non-factorisable **correction to top-quark rapidity** fairly flat for $|y_t| < 2.5$, $\mathcal{O}(0.25\%)$.
2. **Sign change** around $|y_t| \sim 3$
3. Factorisable corrections change sign around $|y_t| \sim 1.2$
4. For some top-quark rapidity values, factorisable and non-factorisable correction become quite comparable.
5. k_t -algorithm to define jets $p_\perp^{jet} > 30\text{GeV}$, $R=0.4$.
6. Non-factorisable corrections reach 1.2 % at $p_\perp^{jet} \sim 140\text{GeV}$.



Conclusions

1. We complete the calculation of **NNLO corrections** to the ***t*-channel single-top production**: the **non-factorisable corrections**.
2. The **auxiliary mass flow method** was used for integral evaluation in VV. It is sufficiently robust to produce results relevant for phenomenology.
3. **Non-factorisable** corrections are **smaller** than, but **quite comparable** to, the **factorisable** ones.
4. If **percent precision** in single-top studies can be reached, the **non-factorisable effects will have to be taken into account**.

Thank you for your attention!

Backup

Double-virtual contribution

The pole structure of the two-loop amplitude is well studied, and can be easily cross-checked against literature

[Catani '98] [Aybat, Dixon, Sterman '06][Becher, Neubert '09][Czakon, Mitov, Sterman '09][Mitov, Sterman, Sung '09, '10][Ferroglia, Neubert, Pecjak, Yang '09]

$$|\mathcal{A}\rangle = \mathbf{Z} |\mathcal{F}\rangle, \quad \mu \frac{d}{d\mu} \mathbf{Z} = -\boldsymbol{\Gamma} \mathbf{Z}$$

$$\Gamma(\{p_i\}, m_i, \mu) = \sum_{(i,j)} \frac{\mathbf{T}_i \cdot \mathbf{T}_j}{2} \gamma_{\text{cusp}}(\alpha_s) \log\left(\frac{\mu^2}{-s_{ij}}\right) + \sum_{(I,j)} \mathbf{T}_I \cdot \mathbf{T}_j \gamma_{\text{cusp}}(\alpha_s) \log\left(\frac{m_I \mu}{-s_{Ij}}\right)$$

Collinear

$$+ \sum_{(I,J)} \frac{\mathbf{T}_I \cdot \mathbf{T}_J}{2} \gamma_{\text{cusp}}(v_{IJ}, \alpha_s) + \sum_i \gamma^i(\alpha_s) + \sum_I \gamma^I(\alpha_s)$$

$n > 1$ massive

$$+ \sum_{(I,J,K)} i f^{abc} T_I^a T_J^b T_K^c F_1(v_{IJ}, v_{JK}, v_{KI}) + \sum_{(I,J)} \sum_k i f^{abc} T_I^a T_J^b T_k^c f_2\left(v_{IJ}, \log\left(\frac{-\sigma_{Jk} v_J \cdot p_k}{-\sigma_{Ik} v_I \cdot p_k}\right)\right) + \mathcal{O}(\alpha_s^3).$$

Non-abelian

Several simplifications occur when only non-factorisable corrections are considered [Brønnum-Hansen, Melnikov, Quarroz, Wang '21]

$$\Gamma_{\text{nf}} = \left(\frac{\alpha_s}{4\pi}\right) \Gamma_{0,\text{nf}} = \left(\frac{\alpha_s}{4\pi}\right) 4 \left[\mathbf{T}_1 \cdot \mathbf{T}_2 \log\left(\frac{\mu^2}{-s - i\epsilon}\right) + \mathbf{T}_2 \cdot \mathbf{T}_3 \log\left(\frac{\mu^2}{-u - i\epsilon}\right) + \mathbf{T}_1 \cdot \mathbf{T}_4 \log\left(\frac{\mu m_t}{m_t^2 - u - i\epsilon}\right) + \mathbf{T}_3 \cdot \mathbf{T}_4 \log\left(\frac{\mu m_t}{m_t^2 - s - i\epsilon}\right) \right]$$

$$\langle \mathcal{A}^{(0)} | \mathcal{A}_{\text{nf}}^{(2)} \rangle = -\frac{1}{8\epsilon^2} \langle \mathcal{A}^{(0)} | \Gamma_{0,\text{nf}}^2 | \mathcal{A}^{(0)} \rangle + \frac{1}{2\epsilon} \langle \mathcal{A}^{(0)} | \Gamma_{0,\text{nf}} | \mathcal{A}_{\text{nf}}^{(1)} \rangle + \langle \mathcal{A}^{(0)} | \mathcal{F}_{\text{nf}}^{(2)} \rangle$$

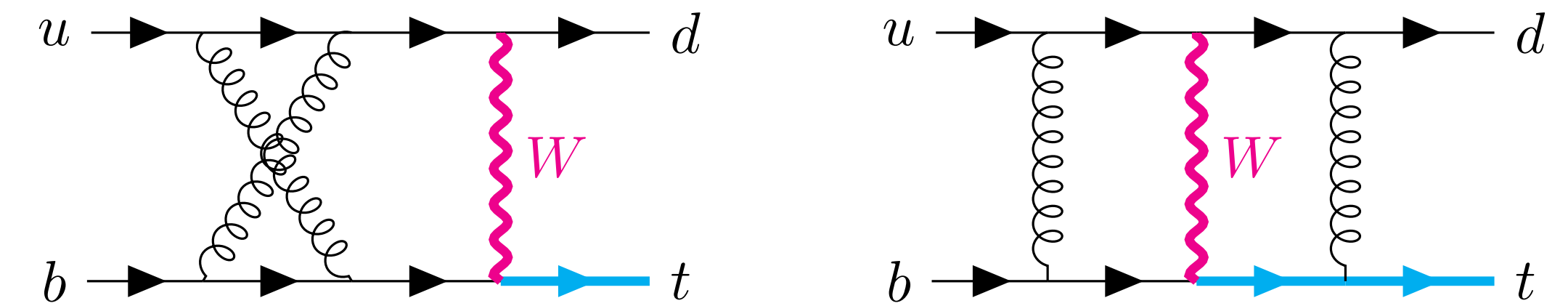
$$\langle \mathcal{A}_{\text{nf}}^{(1)} | \mathcal{A}_{\text{nf}}^{(1)} \rangle = -\frac{1}{4\epsilon^2} \langle \mathcal{A}^{(0)} | |\Gamma_{0,\text{nf}}|^2 | \mathcal{A}^{(0)} \rangle + \frac{1}{2\epsilon} \langle \mathcal{A}_{\text{nf}}^{(1)} | \Gamma_{0,\text{nf}} | \mathcal{A}^{(0)} \rangle + \frac{1}{2\epsilon} \langle \mathcal{A}^{(0)} | \Gamma_{0,\text{nf}}^\dagger | \mathcal{A}^{(1)} \rangle + \langle \mathcal{F}_{\text{nf}}^{(1)} | \mathcal{F}_{\text{nf}}^{(1)} \rangle$$

Double-virtual contribution: amplitude evaluation [Brønnum-Hansen, Melnikov, Quarroz, Wang '21]

Process: $u(p_1) + b(p_2) \rightarrow d(p_3) + t(p_4)$

Kinematic scales: $p_i^2 = 0, i = 1, 2, 3, p_4^2 = m_t^2, s, t, m_W^2$

Dimensions: $d = 4 - 2\epsilon$



Planar and non-planar amplitudes appear at 2-loop order. However, only a particular combination of them do actually contribute

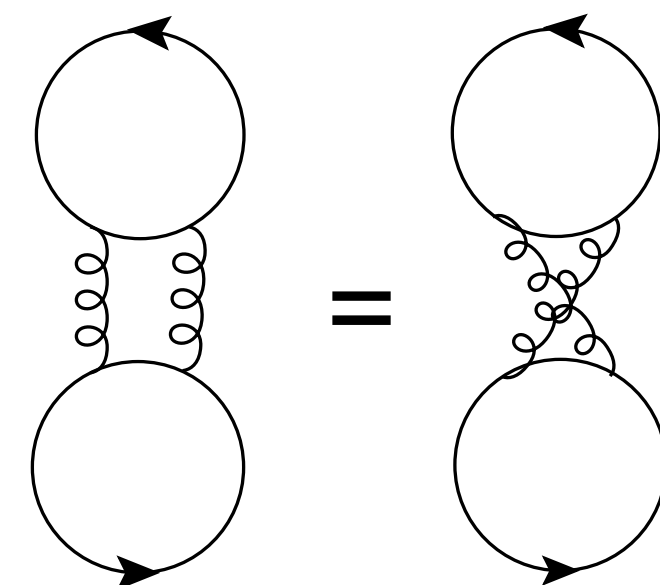
$$\mathcal{A}_{\text{nf}}^{(2)} = \frac{1}{4} \left\{ T^a, T^b \right\}_{c_3 c_1} \left\{ T^a, T^b \right\}_{c_3 c_1} \left(A_{\text{nf}}^{(2), \text{pl}} + A_{\text{nf}}^{(2), \text{npl}} \right) + \dots$$

$$A_{\text{nf}}^{(2)} = A_{\text{nf}}^{(2), \text{pl}} + A_{\text{nf}}^{(2), \text{npl}}$$

Upon interference with tree-level amplitude the colour distinction between planar and non-planar diagrams disappears

(Abelian nature of non-factorisable corrections)

$$\sum_{\text{color}} \mathcal{A}^{(0)*} \mathcal{A}_{\text{nf}}^{(2)} = \frac{1}{4} (N_c^2 - 1) A^{(0)*} A_{\text{nf}}^{(2)*}$$

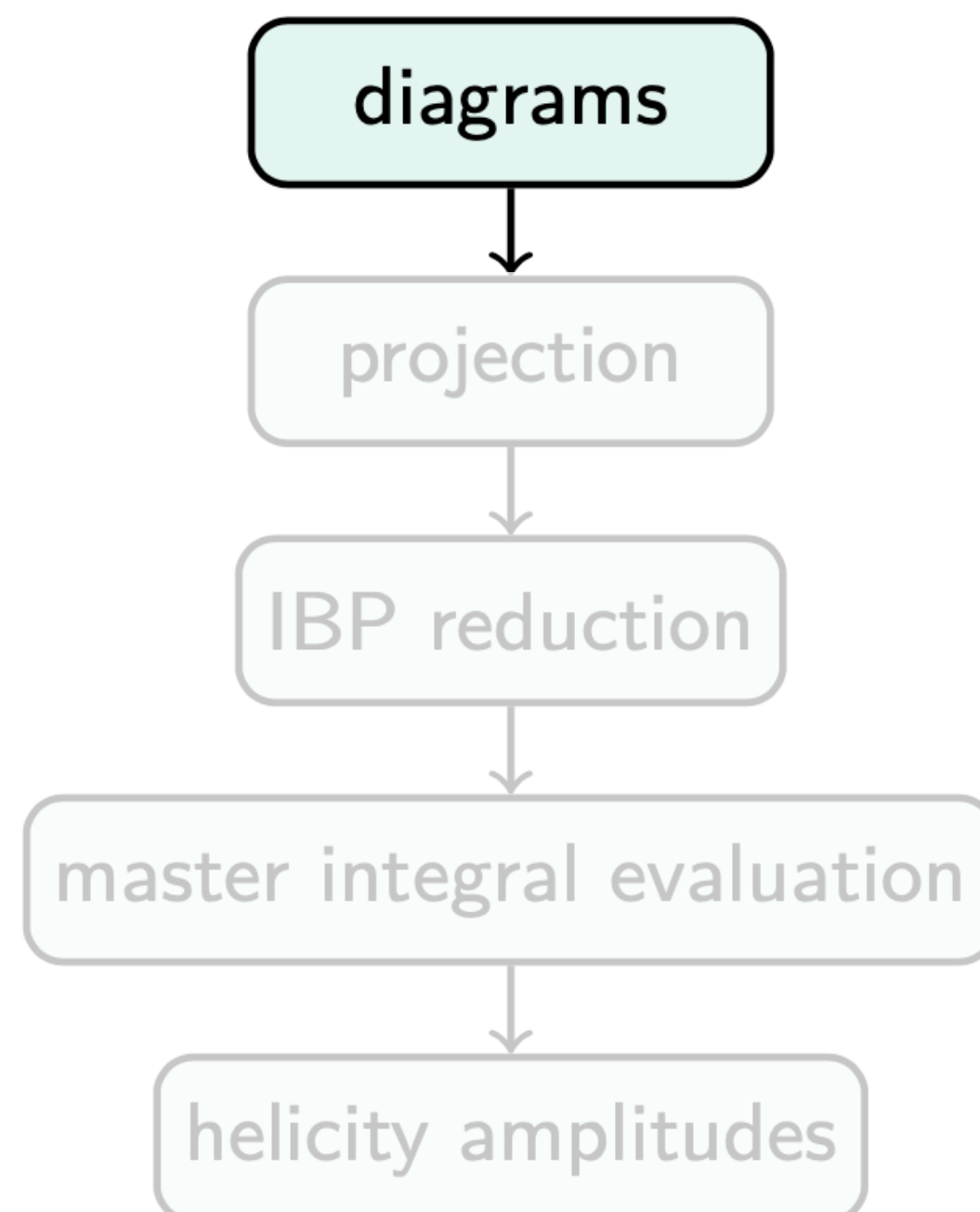
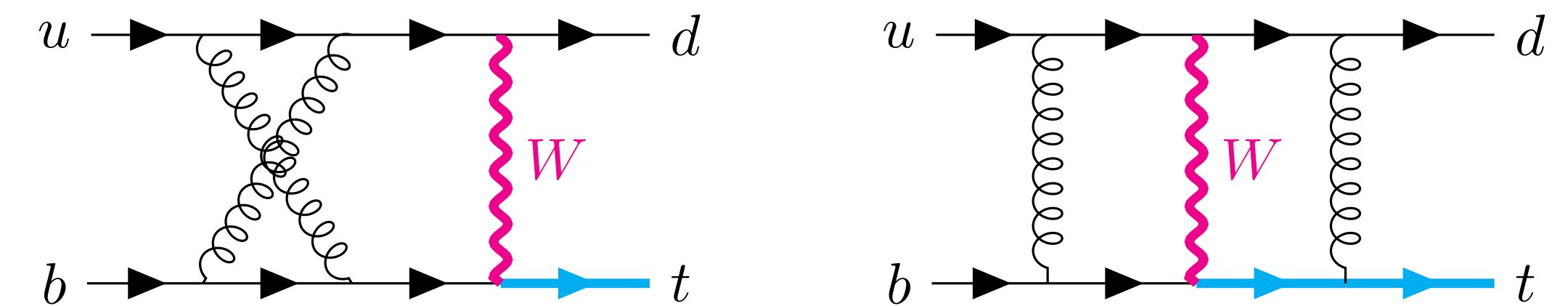


Double-virtual contribution: amplitude evaluation [Brønnum-Hansen, Melnikov, Quarroz, Wang '21]

Process: $u(p_1) + b(p_2) \rightarrow d(p_3) + t(p_4)$

Kinematic scales: $p_i^2 = 0$, $i = 1, 2, 3$, $p_4^2 = m_t^2, s, t, m_W^2$

Dimensions: $d = 4 - 2\epsilon$



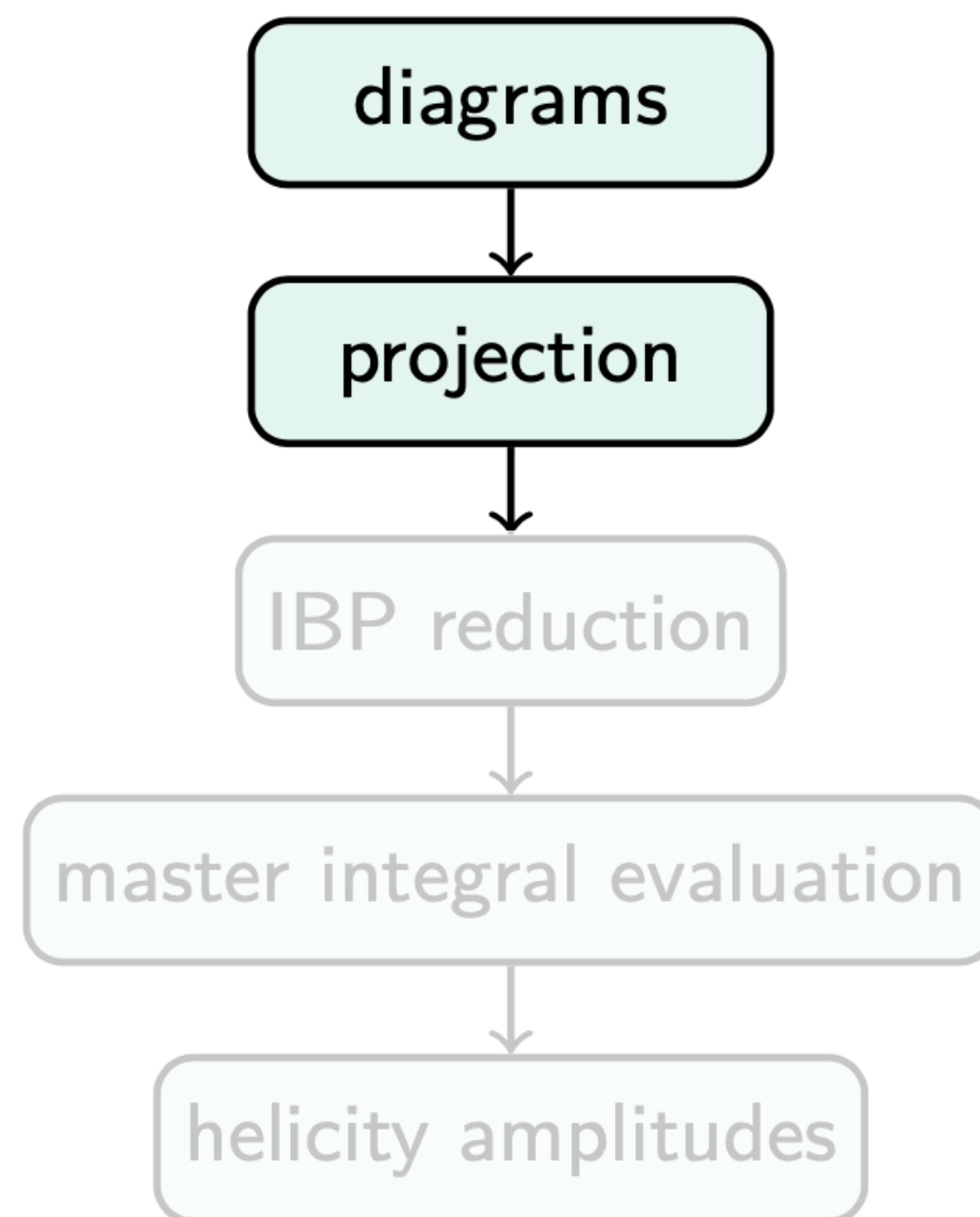
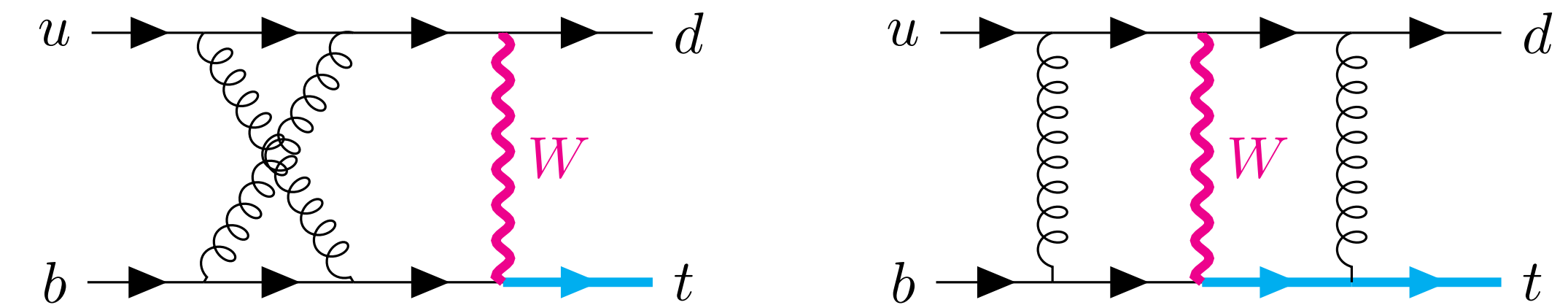
- **18 diagrams**: generated with QGRAF [Nogueira '93] and processed with FORM [Vermaseren '00] [Kuijpers et al. '15] [Ruijl et al. '17]. All **topologies maximal**.

Double-virtual contribution: amplitude evaluation [Brønnum-Hansen, Melnikov, Quarroz, Wang '21]

Process: $u(p_1) + b(p_2) \rightarrow d(p_3) + t(p_4)$

Kinematic scales: $p_i^2 = 0, i = 1, 2, 3,$ $p_4^2 = m_t^2, s, t, m_W^2$

Dimensions: $d = 4 - 2\epsilon$



- One- and two-loop **amplitudes** are written in terms of **invariant form factors** and **independent Lorentz structure**
- γ_5 enters through **charged weak currents** (left-handed projectors)
- Use **anti-commuting prescription** for γ_5 and move **left-handed projectors** to act on external **massless fermions**.
- **11 structures** $\mathcal{S}_i(\lambda)$ and corresponding **form factor (FF)**

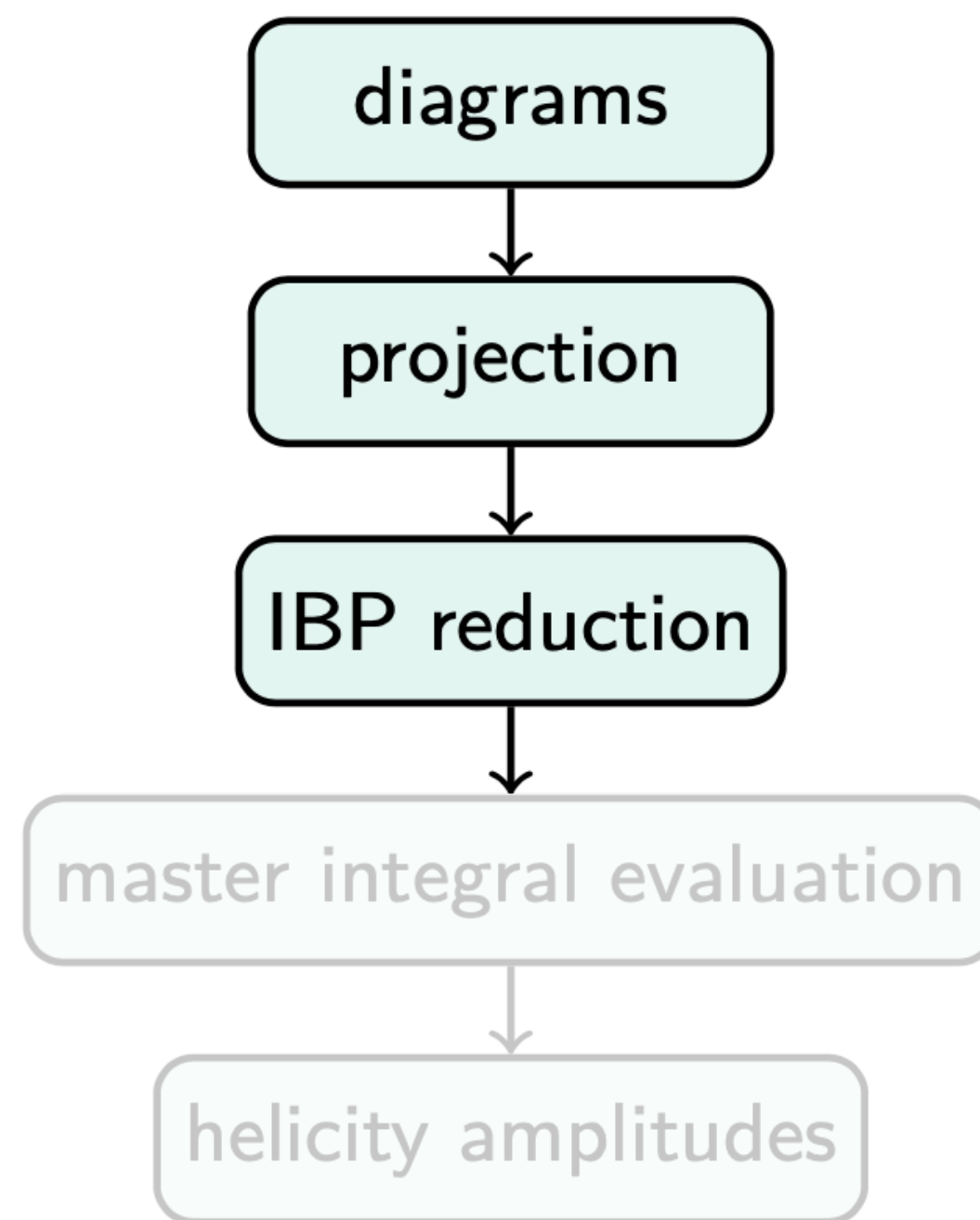
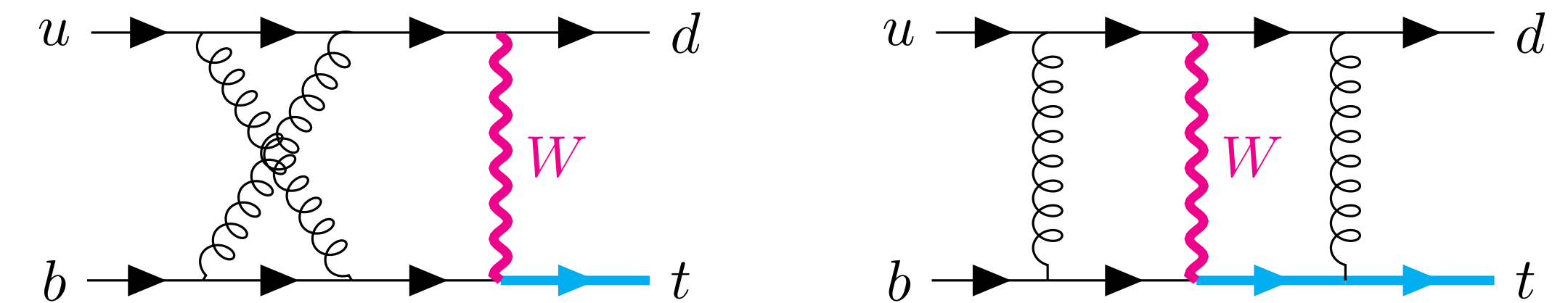
$$Q_i = \sum_{\vec{\lambda}} \mathcal{S}_i^\dagger(\vec{\lambda}) A_{\text{nf}}^{(2)}(\vec{\lambda}), \quad i = 1, \dots, 11$$
- **FF do not depend on helicities of external particles** \rightarrow **vector current part**
- **Polarisation sum** returns independent **traces** \rightarrow scalar products of loop and external momenta (**no external spinor**)

Double-virtual contribution: amplitude evaluation [Brønnum-Hansen, Melnikov, Quarroz, Wang '21]

Process: $u(p_1) + b(p_2) \rightarrow d(p_3) + t(p_4)$

Kinematic scales: $p_i^2 = 0$, $i = 1, 2, 3$, $p_4^2 = m_t^2, s, t, m_W^2$

Dimensions: $d = 4 - 2\epsilon$



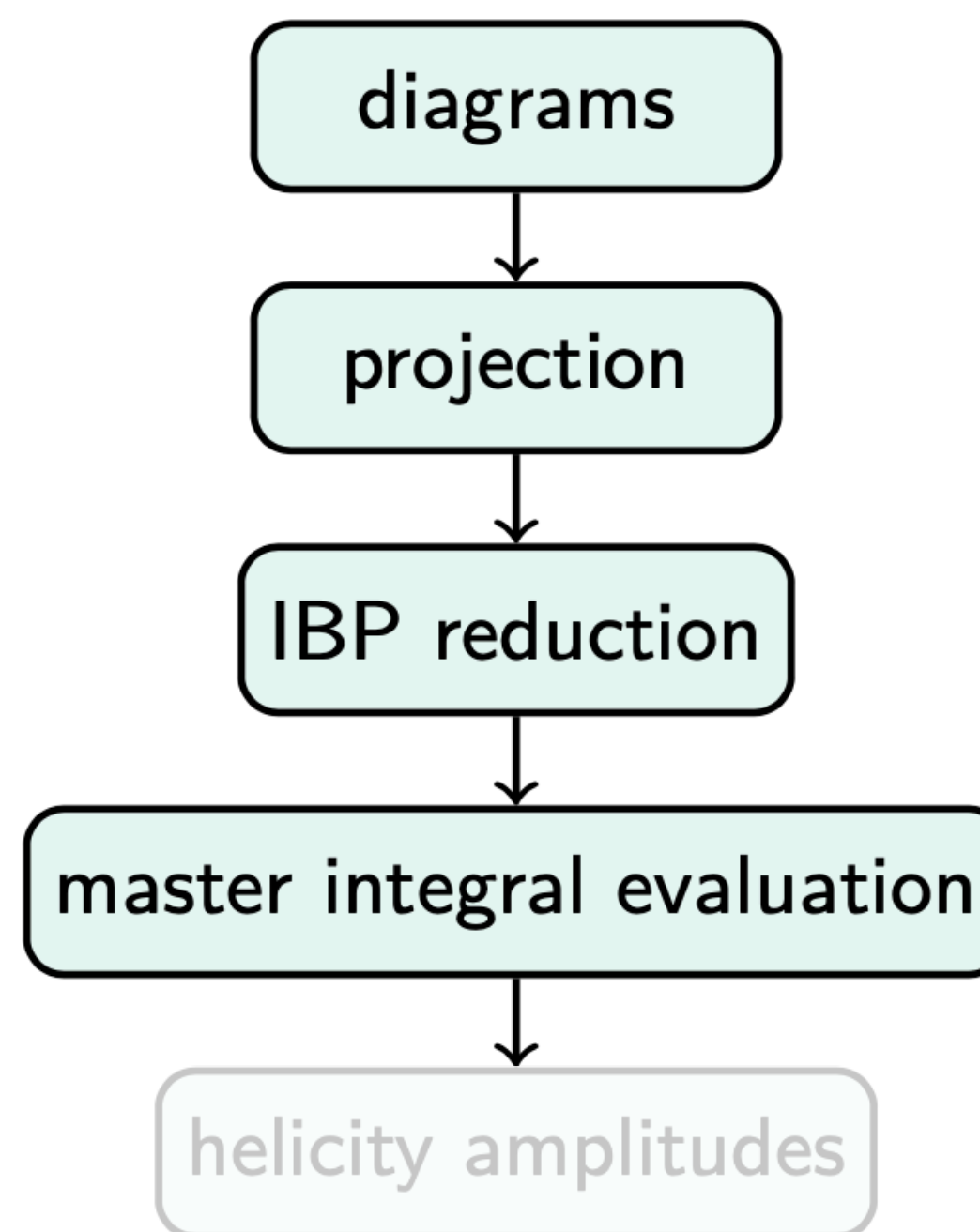
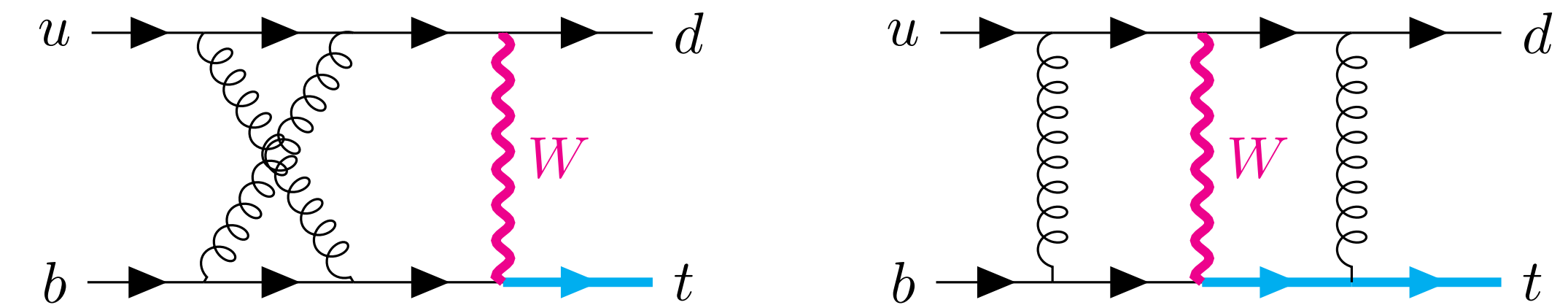
- Reduction performed analytically with KIRA2.0 [Klappert, Lange et al. '20] and FireFly [Klappert, Lange '20] [Klappert, Klein et al. '21]
- $$\langle \mathcal{A}^{(0)} | \mathcal{A}_{\text{nf}}^{(2)} \rangle = \frac{1}{4} (N_c^2 - 1) \sum_{i=1}^{428} c_i(d, s, t, m_t, m_w) I_i$$
- Most complicated took 4 days on 20 cores.
- 428 master integrals I_i .
- Exact dependence on the top-quark mass and the W mass (very first reduction to master integral performed for the fixed numerical relation $m_t^2 = 14/3 m_W^2$ [Assadsolimani et al. '14])

Double-virtual contribution: amplitude evaluation [Brønnum-Hansen, Melnikov, Quarroz, Wang '21]

Process: $u(p_1) + b(p_2) \rightarrow d(p_3) + t(p_4)$

Kinematic scales: $p_i^2 = 0, i = 1, 2, 3, p_4^2 = m_t^2, s, t, m_W^2$

Dimensions: $d = 4 - 2\epsilon$



- Compute **master integrals** using the **auxiliary mass flow method** [Liu, Ma, Wang '18] [Liu, Ma, Tao, Zhang '21]

$$I \propto \lim_{\eta \rightarrow 0^+} \int \prod_{i=1}^2 d^d k_i \prod_{a=1}^9 \frac{1}{[q_a^2 - (m_a^2 - i\eta)]^{\nu_a}}$$

- Add **imaginary part to the W boson mass** $m_W^2 \rightarrow m_W^2 - i\eta$

- **Solve system of DE** at each **phase space point**: $\partial_x I = MI, m_W^2 - i\eta = m_W^2(1 + x)$

- **Boundary condition** $x \rightarrow -i\infty$, **physical point** $x = 0$.

- Some of the **boundary integrals** are **hard to compute**: add **imaginary part to the top mass** $m_t^2 \rightarrow m_t^2 - i\eta$

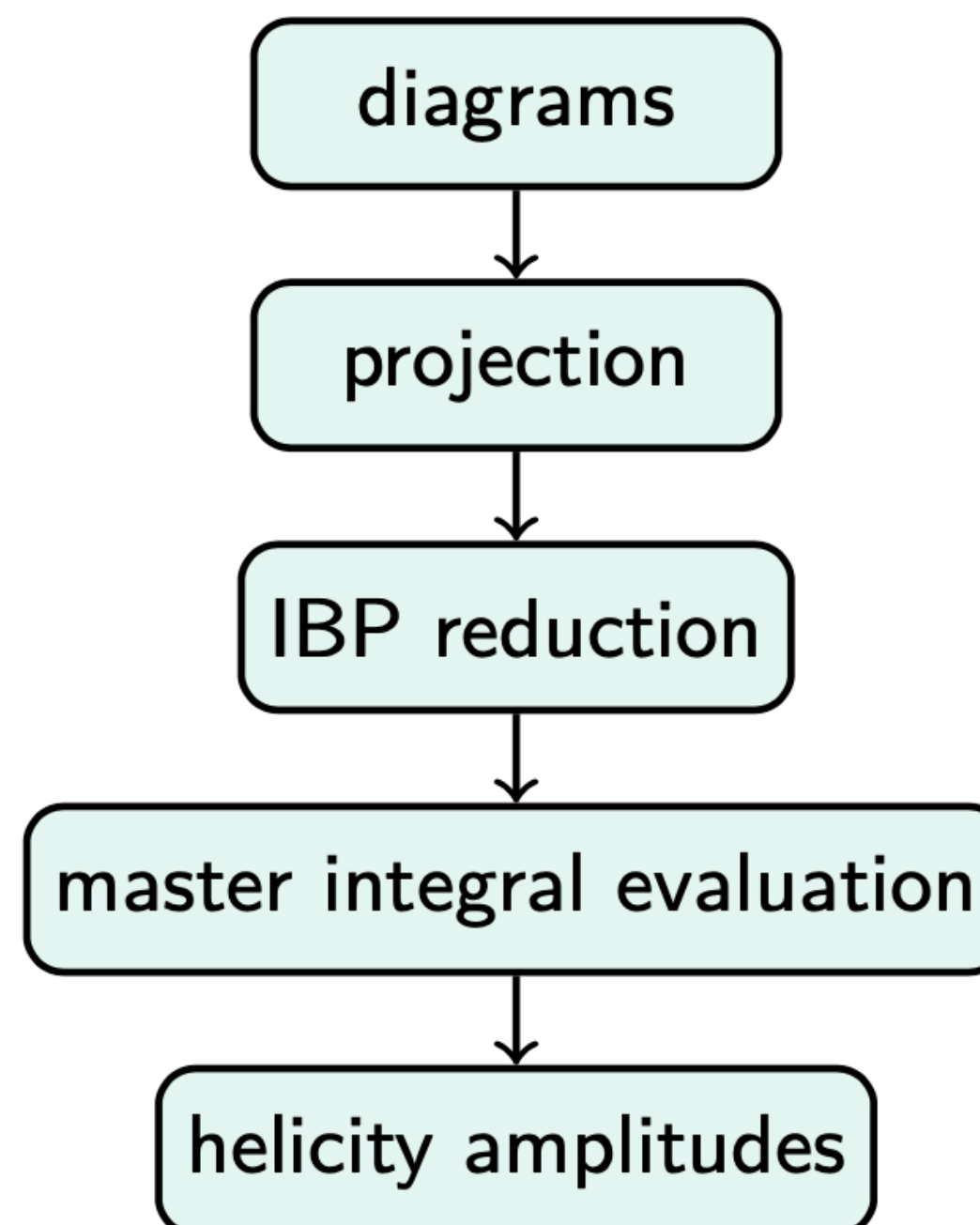
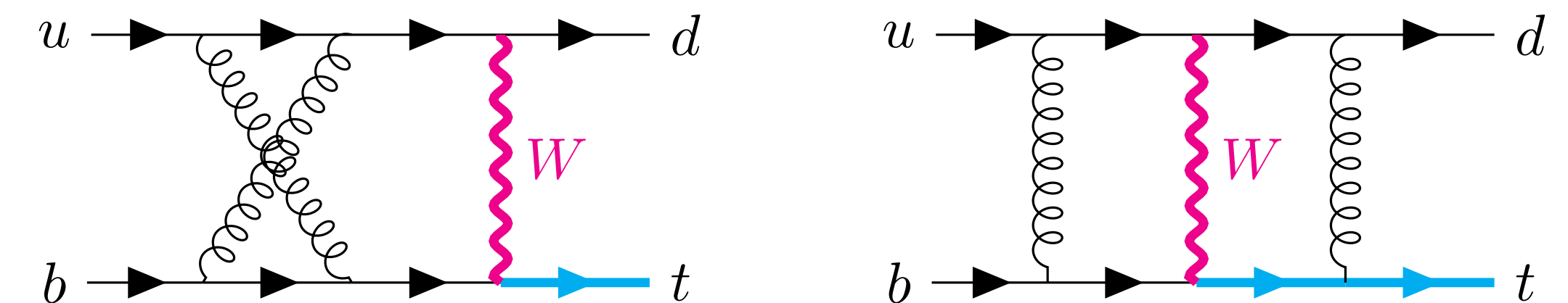
- **DE in m_t . Boundary $\eta \rightarrow \infty$. Physical point $\eta \rightarrow 0$.**

Double-virtual contribution: amplitude evaluation [Brønnum-Hansen, Melnikov, Quarroz, Wang '21]

Process: $u(p_1) + b(p_2) \rightarrow d(p_3) + t(p_4)$

Kinematic scales: $p_i^2 = 0$, $i = 1, 2, 3$, $p_4^2 = m_t^2, s, t, m_W^2$

Dimensions: $d = 4 - 2\epsilon$



- **t'Hooft-Veltman scheme:** external momenta in $d = 4$ and internal momenta in $d = 4 - 2\epsilon$
- To be non-vanishing a matrix events in $d = 4 - 2\epsilon$ between two $d = 4$ spinors requires an even number of matrices with support in -2ϵ space
- ϵ dependence can be explicitly and unambiguously extracted

	7 TeV pp		14 TeV pp		1.96 TeV $p\bar{p}$
	top	anti-top	top	anti-top	$t + \bar{t}$
$\sigma_{\text{LO}}^{\mu=m_t}$	$37.1^{+7.1\%}_{-9.5\%}$	$19.1^{+7.3\%}_{-9.7\%}$	$134.6^{+10.0\%}_{-12.1\%}$	$78.9^{+10.4\%}_{-12.6\%}$	$2.09^{+0.8\%}_{-3.1\%}$
$\sigma_{\text{LO}}^{\text{DDIS}}$	$39.5^{+6.4\%}_{-8.6\%}$	$19.9^{+7.0\%}_{-9.3\%}$	$140.9^{+9.4\%}_{-11.4\%}$	$80.7^{+10.2\%}_{-12.3\%}$	$2.31^{+0.3\%}_{-1.8\%}$
$\sigma_{\text{NLO}}^{\mu=m_t}$	$41.4^{+3.0\%}_{-2.0\%}$	$21.5^{+3.1\%}_{-2.0\%}$	$154.3^{+3.1\%}_{-2.3\%}$	$91.4^{+3.1\%}_{-2.2\%}$	$1.96^{+3.1\%}_{-2.3\%}$
$\sigma_{\text{NLO}}^{\text{DDIS}}$	$41.8^{+3.3\%}_{-2.0\%}$	$21.5^{+3.4\%}_{-1.6\%}$	$154.4^{+3.7\%}_{-1.4\%}$	$91.2^{+3.1\%}_{-1.8\%}$	$2.00^{+3.6\%}_{-3.4\%}$
PDF	$+1.7\%$ -1.4%	$+2.2\%$ -1.5%	PDF +1.7% -1.1%	PDF +1.9% -0.9%	PDF +4.3% -5.3%
$\sigma_{\text{NNLO}}^{\mu=m_t}$	$41.9^{+1.2\%}_{-0.7\%}$	$21.9^{+1.2\%}_{-0.7\%}$	$153.3(2)^{+1.0\%}_{-0.6\%}$	$91.5(2)^{+1.1\%}_{-0.9\%}$	$2.08^{+2.0\%}_{-1.3\%}$
$\sigma_{\text{NNLO}}^{\text{DDIS}}$	$41.9^{+1.3\%}_{-0.8\%}$	$21.8^{+1.3\%}_{-0.7\%}$	$153.4(2)^{+1.1\%}_{-0.7\%}$	$91.2(2)^{+1.1\%}_{-0.9\%}$	$2.07^{+1.7\%}_{-1.1\%}$
PDF	$+1.3\%$ -1.1%	$+1.4\%$ -1.3%	PDF +1.2% -1.0%	PDF +1.0% -1.0%	PDF +3.7% -5.0%

Fully inclusive cross section for pp collision @7TeV and @14TeV (LHC), as well as $p\bar{p}$ collision @1.96TeV (Tevatron) with scales $\mu_R = \mu_F = m_t$ and DDIS scales using CT14 PDFs. [Campbell, Neumann, Sullivan '21]